Title about thermo-electro-mechanics

M. Masó[a,1], R. Ortigosa[b,2], J. Martínez-Frutos[b,3], A. J. Gil[c], M. Barillas[a], A. García-Martínez[a,d], J. Bonet[a,d]

[a] *International Centre for Numerical Methods in Engineering (CIMNE), Barcelona, Spain*
[b] *Computational Mechanics and Scientific Computing Group, Technical University of Cartagena (UPCT), Campus Muralla del Mar, 30202, Cartagena (Murcia), Spain*
[c] *Zienkiewicz Centre for Computational Engineering, College of Engineering Swansea University, Bay Campus, SA1 8EN, United Kingdom*
[d] *Universitat Politècnica de Catalunya (UPC), Barcelona, Spain*

Abstract

Keywords: finite element method, nonlinear thermo-elastodynamics, energy-momentum scheme, structure-preserving discretisation.

1. Introduction

Dielectric Elastomers (DEs) are a class of Electro Active Polymers (EAPs) that have demonstrated remarkable electrically induced actuation properties [33, 37, 44, 45]. These materials are particularly sensitive to changes of the thermal field, but remain frequently unconsidered [8, 18, 21, 25, 56, 58]. Nonetheless, a thermodynamically consistent framework for the simulation of EAPs under non-isothermal conditions was postulated in Reference [57]. In this connection, numerical studies have been recently published [41], where time dependent effects have been restricted to the thermo-viscoelastic behaviour of the material, excluding inertial effects.

Energy-Momentum (EM) time integration schemes are regarded as both elegant and robust because they are endowed by construction with the discrete analogue of the conservation properties of the continuum, namely the conservation of total energy, linear and angular momenta. The *consistency* of EM schemes refers to their ability to preserve (or dissipate for non-reversible constitutive models) the total energy of a system in agreement with the laws of thermodynamics [10, 22, 28, 39]. Consistency of these methods is attained by replacing the (exact) partial derivatives of the Helmholtz free energy functional with respect to its arguments ($\boldsymbol{C}$ and θ) with their carefully designed algorithmic counterparts. These algorithmic partial derivatives, also known as *discrete derivatives* [10, 22, 26, 39, 42, 51], are formulated in compliance with the so-called *directionality property* [26].

Very recently, Franke et. al. [10, 22] have proposed a novel EM scheme in the context of nonlinear elasticity and thermo-elasticity, by taking advantage of the concept of polyconvexity [3–6, 48] and the use of a novel tensor cross product pioneered by de Boer [19] and re-discovered in the context of nonlinear continuum mechanics by Bonet et al. [12–14]. In essence, the authors propose the consideration of four discrete derivatives which are used to form algorithmic versions

[1] Corresponding author: mmaso@cimne.upc.edu
[2] Corresponding author: rogelio.ortigosa@upct.es
[3] Corresponding author: jesus.martinez@upct.es

of the second Piola-Kirchhoff stress tensor and the entropy of the system. In addition to the discrete derivative with respect to the temperature, three further discrete derivatives are presented, which represent the algorithmic counterparts of the work conjugates of the right Cauchy-Green deformation tensor, its co-factor and its determinant. This strategy leads to simplified expressions of the algorithmic second Piola-Kirchhoff stress tensor and entropy, when comparing against those obtained following the classical approach [26]. Furthermore, this work was extended to multi-physics scenarios, such as thermo-elasticity [43], nonlinear electro-mechanics [23, 42] and to thermo-electro-mechanics [24]. The aim of the current paper is the development of a new polyconvexity inspired EM scheme for non-isothermal long-term simulations of DEs, assessing its superiority in terms of long-term stability with respect to other classical time integrators.

The outline of this paper is as follows: in Section 2, some basic principles of kinematics are presented. The governing equations in nonlinear thermo-electro-elastodynamics are also presented in this section. Section 3 delves into mathematical requirements inherent to constitutive models in nonlinear thermo-electro-mechanics. Section 5 presents the weak forms associated with the governing equations in thermo-electro-elastodynamics. These will help introducing the new temperature-based one-step implicit EM time integrator scheme for thermo-elastodynamics in Section 5.3. Section 5.4 briefly describes the finite element implementation of the new time integrator scheme and Section 7 presents a series of numerical examples in order to validate the conservation properties and robustness of the new scheme. Finally, Section 8 provides some concluding remarks. **??** presents an entropy-based EM scheme, counterpart of the temperature-based scheme pursued in this paper. **??** outlines the definition of the discrete derivative expressions featuring in the proposed time integrator in Section 5.3. **??** summarises the EM scheme in Reference [22], illustrating the differences between this and the new EM proposed. **??** presents the steps that need to be carried out in order to derive the thermo-elastic constitutive model presented in Section **??**.

2. Nonlinear continuum thermo-electro-mechanics

A brief introduction into nonlinear continuum mechanics and the relevant governing equations will be presented in this section.

2.1. Kinematics: motion and deformation

Let $\mathcal{B}_0 \subset \mathbb{R}^3$ denote an open, bounded, and connected set representing the reference (undeformed) configuration of an elastic body. The motion of the body is described by a mapping

$$\boldsymbol{\phi} : \mathcal{B}_0 \times \mathbb{R} \to \mathbb{R}^3,$$

assumed to be sufficiently smooth, one-to-one, and orientation preserving. For each material point $\boldsymbol{X} \in \mathcal{B}_0$, the mapping $\boldsymbol{\phi}$ assigns its current position $\boldsymbol{x} \in \mathbb{R}^3$ at time t according to

$$\boldsymbol{x} = \boldsymbol{\phi}(\boldsymbol{X}, t), \qquad \mathcal{B}(t) = \boldsymbol{\phi}(\mathcal{B}_0, t),$$

see Figure 1. The deformation gradient associated with the motion $\boldsymbol{\phi}$ is defined as

$$\boldsymbol{F} : \mathcal{B}_0 \times \mathbb{R} \to \mathbb{R}^{3\times 3}, \qquad \boldsymbol{F} = \boldsymbol{\nabla}_0 \boldsymbol{\phi}(\boldsymbol{X}, t).$$

From $\boldsymbol{F}$, the cofactor tensor $\boldsymbol{H}$ and the Jacobian determinant J are introduced as

$$\boldsymbol{H} = (\det \boldsymbol{F})\, \boldsymbol{F}^{-T} = \frac{1}{2}\, \boldsymbol{F} \times \boldsymbol{F}, \qquad J = \det \boldsymbol{F} = \frac{1}{6}\, (\boldsymbol{F} \times \boldsymbol{F}) : \boldsymbol{F}, \tag{1}$$

where the tensor cross product is defined componentwise by

$$(\boldsymbol{A} \times \boldsymbol{B})_{iI} = \mathcal{E}_{ijk} \mathcal{E}_{IJK} A_{jJ} B_{kK}, \qquad \forall\, \boldsymbol{A}, \boldsymbol{B} \in \mathbb{R}^{3\times 3},$$

and $\mathcal{E}_{ijk}$ (or $\mathcal{E}_{IJK}$) denotes the components of the third-order alternating tensor[4].

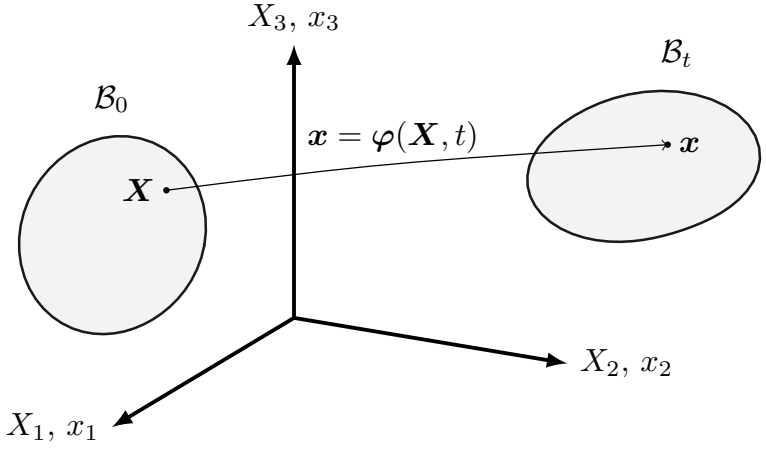

Figure 1: The mapping $\boldsymbol{\phi}$ and the mechanical and thermal portions of the boundary where Dirichlet conditions are imposed in the reference (and deformed) configurations, namely $\partial_{\boldsymbol{\phi}}\mathcal{B}_0$ (and $\partial_{\boldsymbol{\phi}}\mathcal{B}$) and $\partial_{\theta}\mathcal{B}_0$ (and $\partial_{\theta}\mathcal{B}$).

[4]The use of repeated indices implies summation, unless otherwise stated. In addition, lower case and capital case indices $\{i, j, k\}$ and $\{I, J, K\}$ will be used to represent the deformed and reference configurations, respectively.

2.2. Governing equations: conservation of linear momentum and angular momentum

The local form of the conservation of linear momentum [27] can be written as

$$\begin{aligned} \rho_0 \dot{\boldsymbol{v}} - \mathrm{DIV}\left(\boldsymbol{P}\right) - \boldsymbol{f}_0 &= \boldsymbol{0}; && \text{in } \mathcal{B}_0 \times [0,T]\,; \\ \left(\boldsymbol{F}\boldsymbol{S}\right)\boldsymbol{N} &= \boldsymbol{t}_0; && \text{on } \partial_{\boldsymbol{t}}\mathcal{B}_0 \times [0,T]\,; \\ \boldsymbol{\phi} &= \bar{\boldsymbol{\phi}}; && \text{on } \partial_{\boldsymbol{\phi}}\mathcal{B}_0 \times [0,T]\,; \\ \dot{\boldsymbol{\phi}}\Big|_{t=0} &= \dot{\bar{\boldsymbol{\phi}}}; && \text{in } \mathcal{B}_0; \\ \boldsymbol{\phi}|_{t=0} &= \bar{\boldsymbol{\phi}}; && \text{in } \mathcal{B}_0, \end{aligned} \tag{2}$$

where $\rho_0 : \mathcal{B}_0 \to \mathbb{R}^+$ represents the mass density of the continuum in the reference configuration, $\boldsymbol{v}$ the velocity field and $(\dot{\bullet}) := \frac{d(\bullet)}{dt}$ denotes differentiation with respect to time. Furthermore, $\boldsymbol{f}_0$ represents a body force per unit undeformed volume $\mathcal{B}_0$ and $\boldsymbol{t}_0$, the traction force per unit undeformed area applied on $\partial_{\boldsymbol{t}}\mathcal{B}_0 \subset \partial\mathcal{B}_0$, such that $\partial_{\boldsymbol{t}}\mathcal{B}_0 \cup \partial_{\boldsymbol{\phi}}\mathcal{B}_0 = \partial\mathcal{B}_0$ and $\partial_{\boldsymbol{t}}\mathcal{B}_0 \cap \partial_{\boldsymbol{\phi}}\mathcal{B}_0 = \emptyset$. Finally, $\boldsymbol{P}$ represents the first Piola-Kirchhoff stress tensor and the local conservation of angular momentum leads to the well-known tensor condition $\boldsymbol{P}\boldsymbol{F}^T = \boldsymbol{F}\boldsymbol{P}^T$. Finally, T represents the upper bound for the time variable $t \in [0,T]$.

2.3. Governing equations in non-linear thermo-mechanics: Gauss's and Faraday's laws

In the electrostatics case considered, the local form of the Gauss's law can be written in a Lagrangian setting as

$$\begin{aligned} \mathrm{DIV}\boldsymbol{D}_0 - \rho_0^e &= 0; && \text{in } \mathcal{B}_0 \times [0,T] \\ \boldsymbol{D}_0 \cdot \boldsymbol{N} &= -\omega_0^e; && \text{on } \partial_\omega\mathcal{B}_0 \times [0,T]\,. \end{aligned} \tag{3}$$

where $\boldsymbol{D}_0$ is the Lagrangian electric displacement vector, ρ_0^e represents an electric volume charge per unit of undeformed volume $\mathcal{B}_0$ and ω_0^e, the electric surface charge per unit of undeformed area $\partial_\omega\mathcal{B}_0 \in \partial\mathcal{B}_0$. Furthermore, the Faraday's law can be written in a Lagrangian setting as

$$\begin{aligned} \boldsymbol{E}_0 &= -\boldsymbol{\nabla}_0\varphi; && \text{in } \mathcal{B}_0 \times [0,T]\,; \\ \varphi &= \bar{\varphi}; && \text{on } \partial_\varphi\mathcal{B}_0 \times [0,T]\,, \end{aligned} \tag{4}$$

where $\boldsymbol{E}_0$ is the Lagrangian electric field vector and φ, the scalar electric potential. In (4), $\partial_\varphi\mathcal{B}_0 \subset \partial\mathcal{B}_0$ represents the part of the boundary where essential electric potential boundary conditions are applied such that $\partial_\omega\mathcal{B}_0 \cup \partial_\varphi\mathcal{B}_0 = \partial\mathcal{B}_0$ and $\partial_\omega\mathcal{B}_0 \cap \partial_\varphi\mathcal{B}_0 = \emptyset$.

2.4. Governing equations in non-linear thermo-mechanics: conservation of energy

The balance of energy equation can be written as

$$\begin{aligned} \theta\dot{\eta} - \mathcal{D} + \mathrm{DIV}\boldsymbol{Q} - R_\theta &= 0; && \text{in } \mathcal{B}_0 \times [0,T]\,; \\ \boldsymbol{Q} \cdot \boldsymbol{N} &= -Q_\theta; && \text{on } \partial_Q\mathcal{B}_0 \times [0,T]\,; \\ \theta &= \bar{\theta}; && \text{on } \partial_\theta\mathcal{B}_0 \times [0,T]\,; \\ \theta|_{t=0} &= \bar{\theta}; && \text{in } \mathcal{B}_0, \end{aligned} \tag{5}$$

where θ is the absolute temperature field and η and $\boldsymbol{Q}$, the entropy and heat flux per unit undeformed volume $\mathcal{B}_0$, respectively. In addition, R_θ represents the heat source per unit undeformed volume $\mathcal{B}_0$ and Q_θ, the heat source per unit undeformed area applied on $\partial_Q\mathcal{B}_0 \subset \partial\mathcal{B}_0$. In (5), $\partial_\theta\mathcal{B}_0$ represents the part of the boundary $\partial\mathcal{B}_0$ where essential temperature boundary conditions

are applied such that $\partial_Q\mathcal{B}_0 \cup \partial_\theta\mathcal{B}_0 = \partial\mathcal{B}_0$ and $\partial_Q\mathcal{B}_0 \cap \partial_\theta\mathcal{B}_0 = \emptyset$. Furthermore, $\mathcal{D}$ correspond with the dissipation inequality.

With the aim of simplifying the time discretisation of (5), the authors in [**?**] proposed an alternative but equivalent re-expression (at the continuum level) to that in (5) as

$$\begin{aligned} \frac{d}{dt}(\theta\eta) - \dot{\theta}\eta - \mathcal{D} + \mathrm{DIV}\boldsymbol{Q} - R_\theta = 0; &\qquad \text{in } \mathcal{B}_0 \times [0,T]\,; \\ \boldsymbol{Q}\cdot\boldsymbol{N} = -Q_\theta; &\qquad \text{on } \partial_Q\mathcal{B}_0 \times [0,T]\,; \\ \theta = \bar{\theta}; &\qquad \text{on } \partial_\theta\mathcal{B}_0 \times [0,T]\,; \\ \theta|_{t=0} = \bar{\theta}; &\qquad \text{in } \mathcal{B}_0. \end{aligned} \tag{6}$$

In this work we will advocate for (6).

3. Constitutive equations in nonlinear thermo-electro-elasticity

The governing equations presented in Section 2 are coupled by means of a suitable constitutive law. The objective of the following section is to introduce some notions on constitutive laws in thermo-electro-viscoelasticity.

3.1. The free energy density function

The system of PDEs presented in equations (2), (3), (4) and (6) is coupled in a nonlinear fashion through the constitutive response of the material. In the case of electro-thermo-viscoelasticity, the free energy density per unit of undeformed volume, denoted as Ψ, will determine the specific dependence of $\{\boldsymbol{P}, \boldsymbol{D}_0, \eta, \mathcal{D}\}$ as functions of $\{\boldsymbol{F}, \boldsymbol{E}_0, \theta, \boldsymbol{\mathcal{A}}\}$, where $\boldsymbol{\mathcal{A}} = \{\boldsymbol{A}_1, \boldsymbol{A}_2, \ldots, \boldsymbol{A}_{n_{\mathrm{Maxw}}}\}$ represent the collection of internal variables $\boldsymbol{A}_\alpha$, $\alpha = \{1, ..., n_{\mathrm{Maxw}}\}$, and n_{Maxw} the number of Maxwell branches used to model the viscoelastic behaviour of the material. This function Ψ, per unit of undeformed volume, encapsulating the constitutive response of the elastic body $\mathcal{B}_0$, can be defined in terms of the deformation gradient field $\boldsymbol{F}$, the material electric field $\boldsymbol{E}_0$, the temperature field θ and internal variables, namely

$$\Psi = \Psi\left(\boldsymbol{F}, \boldsymbol{E}_0, \theta, \boldsymbol{\mathcal{A}}\right) \tag{7}$$

Using thermodynamical principles, the dissipation inequality $\mathcal{D}$ in the context of thermo-electro-viscoelasticity can be written as

$$\mathcal{D} = \boldsymbol{P} : \dot{\boldsymbol{F}} - \boldsymbol{D}_0 \cdot \dot{\boldsymbol{E}}_0 - \eta\dot{\theta} - \dot{\Psi}\left(\boldsymbol{F}, \boldsymbol{E}_0, \theta, \boldsymbol{\mathcal{A}}\right) \geq 0 \tag{8}$$

where the time derivative of the free energy density $\Psi\left(\boldsymbol{F}, \boldsymbol{E}_0, \theta, \boldsymbol{\mathcal{A}}\right)$ is computed as

$$\dot{\Psi}\left(\boldsymbol{F}, \boldsymbol{E}_0, \theta, \boldsymbol{\mathcal{A}}\right) = \partial_{\boldsymbol{F}}\Psi : \dot{\boldsymbol{F}} + \partial_{\boldsymbol{E}_0}\Psi \cdot \dot{\boldsymbol{E}}_0 + \partial_\theta\Psi\dot{\theta} + \sum_{i=\alpha}^{n_{\mathrm{Maxw}}} \partial_{\boldsymbol{A}_\alpha}\Psi : \dot{\boldsymbol{A}}_\alpha \tag{9}$$

assuming that the internal variables $\boldsymbol{A}_\alpha$ correspond second order tensors. Use of the Coleman and Noll procedure in (8) and (9) yields the following standard constitutive relationships

$$\boldsymbol{P}\left(\boldsymbol{F}, \boldsymbol{E}_0, \theta, \boldsymbol{\mathcal{A}}\right) = \partial_{\boldsymbol{F}}\Psi; \qquad \boldsymbol{D}_0\left(\boldsymbol{F}, \boldsymbol{E}_0, \theta, \boldsymbol{\mathcal{A}}\right) = -\partial_{\boldsymbol{E}_0}\Psi; \qquad \eta\left(\boldsymbol{F}, \boldsymbol{E}_0, \theta, \boldsymbol{\mathcal{A}}\right) = -\partial_\theta\Psi; \tag{10}$$

permitting to simplify the dissipation inequality as

$$\mathcal{D}\left(\boldsymbol{F}, \boldsymbol{E}_0, \theta, \boldsymbol{\mathcal{A}}\right) = -\sum_{i=\alpha}^{n_{\mathrm{Maxw}}} \partial_{\boldsymbol{A}_\alpha}\Psi : \dot{\boldsymbol{A}}_\alpha \tag{11}$$

In this section we will present the specific form of the energy density function encapsulating the constitutive coupled thermo-electro-mechanical response of the continuum $\mathcal{B}_0$, emphasising on the mathematical/physical constraints that this need to comply with.

3.2. Thermal variation and third law of thermodynamics

The Third Law of thermodynamics establishes that "the entropy of a body should be zero at Kelvin state (zero temperature)", namely

$$\lim_{\theta\to 0}\eta = 0\,. \tag{12}$$

In addition, the specific heat coefficient, denoted as c_v and defined as

$$c_v(\boldsymbol{F},\boldsymbol{E}_0,\theta,\mathcal{A}) = -\theta\frac{\partial^2\Psi}{\partial\theta\partial\theta} = \theta\frac{\partial\eta}{\partial\theta} \tag{13}$$

must be strictly positive ($c_v > 0$) to ensure material stability, which implies that the free energy density Ψ must be concave with respect to the temperature ($\partial^2_{\theta\theta}\Psi < 0$). Furthermore, at the reference unstressed configuration, it must recover the reference specific heat coefficient c_v^0. To circumvent this and ensure strict compliance with the Third Law of Thermodynamics, we adopt the formulation recently proposed by Bonet and Gil [16].

In order to develop a complete constitutive model, an assumtion of independence between the thermal variation and the mechanical and electrical physics is made, which is common in the literature, considering a multiplicative decomposition as

$$c_v(\boldsymbol{F},\boldsymbol{E}_0,\theta,\mathcal{A}) = c_v^0\mathcal{X}(\boldsymbol{F},\boldsymbol{E}_0,\mathcal{A})g(\theta) \tag{14}$$

where c_v^0 is the specific heat coefficient at the reference configuration, $\mathcal{X}(\boldsymbol{F},\boldsymbol{E}_0,\mathcal{A})$ is a dimensionless function that captures the dependence of the specific heat coefficient with the mechanical and electrical physics, and $g(\theta)$ is a purely thermal function that captures the temperature dependence of the specific heat coefficient.

Later, a generalised form of the specific heat based on an additive decomposition, will be adopted to model different thermal responses or components as

$$c_v(\boldsymbol{F},\boldsymbol{E}_0,\theta,\mathcal{A}) = \sum_{i=1}^{n} c_v^i\mathcal{X}^i(\boldsymbol{F},\boldsymbol{E}_0,\mathcal{A})g^i(\theta) \quad ; \qquad \sum_{i=1}^{n} c_v^i\mathcal{X}(\boldsymbol{I},\boldsymbol{0},\boldsymbol{0}) = c_v^0\,. \tag{15a,b}$$

Integration of the specific heat coefficient in (13) with respect to temperature after having substituted the multiplicative decomposition in (14) allows to obtain the following expression for the entropy:

$$\eta(\boldsymbol{F},\boldsymbol{E}_0,\theta,\mathcal{A}) = \eta_R(\boldsymbol{F},\boldsymbol{E}_0,\mathcal{A})\left(1+\frac{1}{\xi_R}\int_{\theta_R}^{\theta}\frac{g(\vartheta)}{\vartheta}\,d\vartheta\right), \tag{16}$$

with

$$\eta_R(\boldsymbol{F},\boldsymbol{E}_0,\mathcal{A}) = c_v^0\mathcal{X}(\boldsymbol{F},\boldsymbol{E}_0,\mathcal{A})\xi_R \quad \text{and} \qquad \xi_R = \int_0^{\theta_R}\frac{g(\vartheta)}{\vartheta}\,d\vartheta\,. \tag{17a,b}$$

Subsequent integration with respect to the temperature yields the following free energy density relation,

$$\Psi(\boldsymbol{F},\boldsymbol{E}_0,\theta,\mathcal{A}) = \Psi_R(\boldsymbol{F},\boldsymbol{E}_0,\mathcal{A}) - \eta_R(\boldsymbol{F},\boldsymbol{E}_0,\mathcal{A})\left(\Delta\theta+\frac{1}{\xi_R}\int_{\theta_R}^{\theta}g(\vartheta)\left(\frac{\theta}{\vartheta}-1\right)d\vartheta\right). \tag{18}$$

More details on the relation between the reference energy Ψ_R and the Kelvin state Ψ_K can be found in [16].

Rearranging terms and using the Legendre transformation, expressions (18) and (16) can by rewritten in the following compact forms,

$$\eta(\boldsymbol{F}, \boldsymbol{E}_0, \theta, \mathcal{A}) = \eta_R(\boldsymbol{F}, \boldsymbol{E}_0, \mathcal{A}) G(\theta)\,, \tag{19a}$$

$$\Psi(\boldsymbol{F}, \boldsymbol{E}_0, \theta, \mathcal{A}) = \mathcal{E}_R(\boldsymbol{F}, \boldsymbol{E}_0, \mathcal{A}) - \theta_R \eta_R(\boldsymbol{F}, \boldsymbol{E}_0, \theta, \mathcal{A}) f(\theta)\,, \tag{19b}$$

with the thermal variations

$$G(\theta) = 1 + \frac{1}{\xi_R} \int_{\theta_R}^{\theta} \frac{g(\vartheta)}{\vartheta} d\vartheta\,, \tag{20a}$$

$$f(\theta) = \frac{\theta}{\theta_R} + \frac{1}{\theta_R \xi_R} \int_{\theta_R}^{\theta} g(\vartheta) \left(\frac{\theta}{\vartheta} - 1 \right) d\vartheta\,. \tag{20b}$$

Particular choices of the coupling functions $\mathcal{E}_R$, η_R and g will define the different types of behaviour of the material, mechanical and electro-mechanical and its thermal variation. In the following section, it will be specified for each term contributing to the free energy density.

3.3. Free energy density decomposition

Once the thermal variation has been uncoupled from the electro-mechanical response, the contributions to the free energy density at the reference temperature, can be decomposed into electrical and mechanical parts. For the purely mechanical part of the material, we will distignuish betweent the volumetric ad isochoric contributions to the free enegy density, as well as the entroy and specific heat, denoted as $\bar{\bullet}$ and $\hat{\bullet}$ respectively for each property. The free energy density at reference temperature can be read as

$$\Psi_R(\boldsymbol{F}, \boldsymbol{E}_0, \mathcal{A}) = \bar{\Psi}_R(J) + \hat{\Psi}_R(\boldsymbol{F}, \mathcal{A}) + \Psi_{R,\text{elec}}(\boldsymbol{F}, \boldsymbol{E}_0) \tag{21}$$

3.3.1. Volumetric free energy density

The pair of functions $\mathcal{E}_R$ amd η_R presented in [17] are convex and concave functions satisfying stability conditions,

$$\bar{\eta}_R(J) = c_v^0 \xi_R + c_v^0 \Gamma \frac{J^q - 1}{q} \tag{22}$$

$$\bar{\mathcal{E}}_R(J) = U(J) + \beta(J-1)\,; \quad U(J) = \frac{1}{2} \kappa_R (J-1)^2\,. \tag{23}$$

The parameter κ_R is the bulk modulus and its corresponding volmetric energy contribution could be replaced by other suitable formulation [55]. q is a dimensionless parameter and β is related with the Mie-Grüneisen constant Γ by imposing null pressure at the reference configuration,

$$\left. \frac{\partial \bar{\Psi}}{\partial J} \right|_{J=1, \theta=\theta_R} = 0 \iff \beta = \Gamma c_v^0 \theta_R\,. \tag{24}$$

The parameter Mie-Grüneisen can also been related with the linear thermal expansion coefficient with the relation

$$\left. \frac{\partial^2 \Psi}{\partial J \partial \theta} \right|_{J=1, \theta=\theta_R} = -3\alpha\kappa_R = -\Gamma c_v^0\,. \tag{25}$$

3.3.2. Isochoric free energy density

Assuming that all the free energy $\mathcal{E}$ is volumetric, the choice $\hat{\Psi}_R = -\theta_R \hat{\eta}_R$ allows simplification of Eq. (19b) as

$$\hat{\Psi}(\boldsymbol{F}, \theta, \mathcal{A}) = \hat{\Psi}(\boldsymbol{F}, \mathcal{A}) f(\theta)\,, \tag{26}$$

which facilitates using standard constitutive models from literature. Usually, the deviatoric free energy density is expressed as the additive decomposition of the hyperelastic and viscous contributions, namely, a generalized Maxwell model. The viscoelastic free energy at reference temperature will read

$$\hat{\Psi}_R(\boldsymbol{F}, \mathcal{A}) = \hat{\Psi}_{R,\infty}(\boldsymbol{F}) + \sum_{\alpha=1}^{n_{\text{Maxw}}} \hat{\Psi}_{R,\alpha}(\boldsymbol{F}, \boldsymbol{A}_\alpha) \tag{27}$$

A possible example for $\hat{\Psi}_{R,\infty}$ is the non-linear Mooney-Rivlin model,

$$\hat{\Psi}_{R,\infty}(\boldsymbol{F}) = \frac{\mu_1}{2\alpha_1 3^{(\alpha_1-1)}}((\boldsymbol{F}:\boldsymbol{F})^{\alpha_1} - 3^{\alpha_1}) + \frac{\mu_2}{2\alpha_2 3^{(\alpha_2-1)}}((\boldsymbol{H}:\boldsymbol{H})^{\alpha_2} - 3^{\alpha_2})\,. \tag{28}$$

In the later section 6 will be discussed some detail about this choice. It's important to note the dependance on the second invariant, which offers a robust representaion of elastomeric materials.

As for the viscous contributions $\hat{\Psi}_{R,\alpha}$, these are based on the evolution of internal state variables $\mathcal{A}$, which will be detailed in Section 3.8. In this upcoming section, the finite strain viscoelasticity model and its associated evolution laws will be described, based on a multiplicative decomposition of the deformation gradient, designed to guarantee positive viscous dissipation and comply with the second law of thermodynamics.

3.3.3. Electro-mechanical coupling

$$\Psi_{R,\text{elec}}(\boldsymbol{F}, \boldsymbol{E}_0) = -\frac{\varepsilon_r \varepsilon_0}{2J} \boldsymbol{H}\boldsymbol{E}_0 \cdot \boldsymbol{H}\boldsymbol{E}_0 \tag{29}$$

3.3.4. Thermal functions

The triplet of functions g_i, G_i and f_i determine the thermal coupling for each component. Once one of the three functions is specified, the remaining ones are uniquely determined via Eqs. (20a) and (20b). As an example, [17] proposes the choice of

$$\bar{g}(\theta) = \left(\frac{\theta}{\theta_R}\right)^{\bar{\gamma}} \;; \quad \bar{\gamma} > 0 \tag{30a,b}$$

where the positivity of the parameter γ is enforced to guarantee the positivity of the specific heat coefficient. In this work, different families of thermal functions will be employed, following the general definition in Eq. (15). While expression (30) is a good choice for the volumetric part, a different family of functions will be employed to capture the non-linear softening of the deviatoric energy. Hence, the following set of functions will be reused in the later section 6, in combination with (30),

$$\hat{f}(\theta) = \frac{1}{\xi_T} \exp\left(-\left(\frac{\theta}{\theta_T}\right)^{\hat{\gamma}}\right)\,, \tag{31a}$$

$$\hat{G}(\theta) = -\frac{\hat{\gamma}}{\xi_T}\frac{\theta_R}{\theta}\left(\frac{\theta}{\theta_T}\right)^{\hat{\gamma}} \exp\left(-\left(\frac{\theta}{\theta_T}\right)^{\hat{\gamma}}\right)\,, \tag{31b}$$

$$\hat{g}(\theta) = \hat{G}(\theta)\left(\hat{\gamma} - \hat{\gamma}\left(\frac{\theta}{\theta_T}\right)^{\hat{\gamma}} - 1\right), \tag{31c}$$

with

$$\xi_T = \exp\left(-\left(\frac{\theta_R}{\theta_T}\right)^{\hat{\gamma}}\right), \quad \hat{\gamma} > 0\,. \tag{32a,b}$$

NOTE: $G = \theta_R\,\partial_\theta f$; $\quad g = \theta\,\partial_\theta G = \theta\theta_R\,\partial_{\theta\theta} f$

$$f = \frac{1}{\xi_T}\exp\left(-\left(\frac{\theta}{\theta_T}\right)^{\gamma}\right)$$
$$f' = -\frac{\gamma}{\xi_T\theta}\left(\frac{\theta}{\theta_T}\right)^{\gamma}\exp\left(-\left(\frac{\theta}{\theta_T}\right)^{\gamma}\right)$$
$$f'' = \frac{\partial f}{\theta}\left(\gamma - \gamma\left(\frac{\theta}{\theta_T}\right)^{\gamma} - 1\right)$$

NOTE: Eq. (31b) evaluates to $\gamma(\theta_R/\theta_T)^\gamma$ at θ_R, which is in contradiction with Eqs. (16) and (20), that state G should be equal to 1 at θ_R.
The origin of this contradiction is the imposition of $\Psi_R = -\theta_R\eta_R$.

Regarding the function $\bar{g} = (\theta/\theta_R)^{\bar{\gamma}}$ (30), the same proportionality constraint presents several difficulties.

For any arbitrary property considered at two different temperatures, there is an inherent proportionality that is independent of the observer's reference temperature. Consequently, two functions g (or the corresponding f) related to different reference temperatures are proportional. For the family of functions defined in (30),

$$\left(\frac{\theta}{\theta_{R_A}}\right)^{\gamma_A} \propto \left(\frac{\theta}{\theta_{R_B}}\right)^{\gamma_B}, \ \forall\,\theta \in \mathbb{R}^+\,.$$

This relation holds if and only if $\gamma_A = \gamma_B = \gamma$. The proportionality constant is then defined by the ratio of the reference temperatures $(\theta_{R_A}/\theta_{R_B})^\gamma$.

The same logic applies to all the families of functions, such as those in (31). As a consequence, the relation between Ψ_R and η_R cannot be specified until a specific thermal function has been chosen.

Let θ_T be the parameter governing the transition temperature of the material properties, and $\hat{\gamma}$ the parameter defining the gradient of that change.

In Section 6 specific values for the families of thermal laws will be presented, as well as the satisfaction of the stability conditions presented in the following section.

3.4. Mathematical and physical constraints in the model

Material stability: In the absence of dissipation, the free energy density must comply with the following mathematical requirements

$$(\boldsymbol{u}\otimes\boldsymbol{V}) : \partial^2_{\boldsymbol{F}\boldsymbol{F}}\Psi : (\boldsymbol{u}\otimes\boldsymbol{V}) > 0; \qquad \boldsymbol{U}\cdot\partial^2_{\boldsymbol{E}_0\boldsymbol{E}_0}\Psi\,\boldsymbol{U} < 0; \qquad \forall\boldsymbol{F}, \boldsymbol{E}_0, \theta \text{ and } \boldsymbol{\mathcal{A}} \tag{33}$$

where $\boldsymbol{u}$, $\boldsymbol{U}$, $\boldsymbol{V} \in \mathbb{R}^3$. The first two conditions in (33) ensure that in the reversible isothermal case, material stability is guaranteed [49], namely, perturbations according to the following ansatzs $\boldsymbol{\Delta\phi} = \boldsymbol{u}\mathcal{G}\left(\boldsymbol{X}\cdot\boldsymbol{V} - c_\alpha t\right)$ and $\Delta\varphi = b\mathcal{F}\left(\boldsymbol{X}\cdot\boldsymbol{U} - c_\alpha t\right)$ admit real solutions for the speed of propagation c_α of the perturbations.

In order to ensure conditions in equation (33), two sufficient conditions are:

$$(\boldsymbol{u}\otimes\boldsymbol{V}) : \partial^2_{\boldsymbol{FF}}\hat{\Psi}_{R,\infty}(\boldsymbol{F},\boldsymbol{E}_0) : (\boldsymbol{u}\otimes\boldsymbol{V}) > 0; \qquad \boldsymbol{U}\cdot\partial^2_{\boldsymbol{E}_0\boldsymbol{E}_0}\hat{\Psi}_{R,\infty}(\boldsymbol{F},\boldsymbol{E}_0)\,\boldsymbol{U} < 0 \tag{34a}$$

$$(\boldsymbol{u}\otimes\boldsymbol{V}) : \partial^2_{\boldsymbol{FF}}\bar{\Psi}_R(J) : (\boldsymbol{u}\otimes\boldsymbol{V}) > 0; \qquad (\boldsymbol{u}\otimes\boldsymbol{V}) : \partial^2_{\boldsymbol{FF}}\bar{\eta}_R(J) : (\boldsymbol{u}\otimes\boldsymbol{V}) > 0 \tag{34b}$$

$$\bar{g}(\theta) > 0,\ \forall\theta\in\mathbb{R}^+; \qquad \hat{g}(\theta) > -1,\ \forall\theta\in\mathbb{R}^+ \tag{34c}$$

First, we will establish sufficient conditions that guarantee the first two conditions over $\hat{\Psi}_{R,\infty}$. Notice that the two conditions affecting $\hat{\Psi}_{R,\infty}$ entail rank-one convexity condition with respect to the mechanical physics and concavity with respect the electric field $\boldsymbol{E}_0$. The definition of free energy densities $\hat{\Psi}_{R,\infty}$ that comply *ab initio* simultaneously with the convexity and concavity conditions in (34a) is far from simple. Instead, a more amenable strain energy density, denote as $\hat{e}_{R,\infty}(\boldsymbol{F},\boldsymbol{D}_0)$ is introduced in order to facilitate the fulfilment of the convexity/concavity constraints of $\hat{\Psi}_{R,\infty}(\boldsymbol{F},\boldsymbol{E}_0)$. The strain energy density $\hat{e}_{R,\infty}(\boldsymbol{F},\boldsymbol{D}_0)$ is related with $\hat{\Psi}_{R,\infty}(\boldsymbol{F},\boldsymbol{E}_0)$ by means of the following standard Legendre transformation

$$\hat{\Psi}_{EM}(\boldsymbol{F},\boldsymbol{E}_0) = \min_{\boldsymbol{D}_0}\{e_R(\boldsymbol{F},\boldsymbol{D}_0) - \boldsymbol{E}_0\cdot\boldsymbol{D}_0\}. \tag{35}$$

It was shown by the authors in XXX that a sufficient condition for $\hat{\Psi}_{R,\infty}$ to satisfy the condition in (34a) is its polyconvexity, namely, $\hat{e}_R(\boldsymbol{F},\boldsymbol{D}_0)$ must be expressed as a convex multi-variable expression, denoted as $\hat{\mathbb{W}}_R$, with respect to the fields $\boldsymbol{\mathcal{V}} = \{\boldsymbol{F},\boldsymbol{H},J,\boldsymbol{D}_0,\boldsymbol{d}\}$, with $\boldsymbol{d} = \boldsymbol{F}\boldsymbol{D}_0$, namely

$$\hat{e}_R(\boldsymbol{F},\boldsymbol{D}_0) = \hat{\mathbb{W}}_R(\boldsymbol{\mathcal{V}}); \qquad \boldsymbol{\mathcal{V}} = \{\boldsymbol{F},\boldsymbol{H},J,\boldsymbol{D}_0,\boldsymbol{d}\},\ \boldsymbol{d} = \boldsymbol{F}\boldsymbol{D}_0 \tag{36}$$

For sufficiently differentiable functions, polyconvexity of $\hat{e}_R$ is equivalent to positive definiteness of the Hessian operator of $\hat{\mathbb{W}}_R(\boldsymbol{\mathcal{V}})$, namely

$$\delta\boldsymbol{\mathcal{V}} : [\mathbb{H}_{\hat{W}_R}] : \delta\boldsymbol{\mathcal{V}} > 0,\ \forall\delta\boldsymbol{\mathcal{V}}, \tag{37}$$

where $[\mathbb{H}_{\hat{W}_R}]$ denotes the (positive definite) Hessian operator of $\hat{W}_R(\boldsymbol{\mathcal{V}})$, namely

$$[\mathbb{H}_{\hat{W}_R}] = \begin{bmatrix} \partial^2_{\boldsymbol{FF}}\hat{W}_R & \partial^2_{\boldsymbol{FH}}\hat{W}_R & \partial^2_{\boldsymbol{F}J}\hat{W}_R & \partial^2_{\boldsymbol{FD}_0}\hat{W}_R & \partial^2_{\boldsymbol{Fd}}\hat{W}_R \\ \partial^2_{\boldsymbol{HF}}\hat{W}_R & \partial^2_{\boldsymbol{HH}}\hat{W}_R & \partial^2_{\boldsymbol{H}J}\hat{W}_{EM} & \partial^2_{\boldsymbol{HD}_0}\hat{W}_R & \partial^2_{\boldsymbol{Hd}}\hat{W}_R \\ \partial^2_{J\boldsymbol{F}}\hat{W}_R & \partial^2_{J\boldsymbol{H}}\hat{W}_R & \partial^2_{JJ}\hat{W}_{EM} & \partial^2_{J\boldsymbol{D}_0}\hat{W}_R & \partial^2_{J\boldsymbol{d}}\hat{W}_R \\ \partial^2_{\boldsymbol{D}_0\boldsymbol{F}}\hat{W}_R & \partial^2_{\boldsymbol{D}_0\boldsymbol{H}}\hat{W}_R & \partial^2_{\boldsymbol{D}_0J}\hat{W}_R & \partial^2_{\boldsymbol{D}_0\boldsymbol{D}_0}\hat{W}_R & \partial^2_{\boldsymbol{D}_0\boldsymbol{d}}\hat{W}_R \\ \partial^2_{\boldsymbol{dF}}\hat{W}_R & \partial^2_{\boldsymbol{dH}}\hat{W}_R & \partial^2_{\boldsymbol{d}J}\hat{W}_R & \partial^2_{\boldsymbol{dD}_0}\hat{W}_R & \partial^2_{\boldsymbol{dd}}\hat{W}_R \end{bmatrix}. \tag{38}$$

A possible definition for $\hat{e}_R(\boldsymbol{F},\boldsymbol{D}_0)$ complying with the polyconvexity condition in (36) is the following

$$\hat{e}_R(\boldsymbol{F},\boldsymbol{D}_0) = \hat{\mathbb{W}}_R(\boldsymbol{F},\boldsymbol{H},J\boldsymbol{D}_0,\boldsymbol{d}) = \frac{\mu_1}{2}II_{\hat{\boldsymbol{F}}} + \frac{\mu_2}{2}II^{3/2}_{\hat{\boldsymbol{H}}} + \frac{1}{2\varepsilon_2 J}II_{\boldsymbol{d}}; \qquad \mu_1,\mu_2,\lambda > 0 \tag{39}$$

which is indeed an additive decomposition between of an isochoric Mooney-Rivlin model (purely mechanical contribution) and an ideal dielectric elastomer model (coupled contribution). Notice that in above model, the isochoric invariants $II_{\hat{\boldsymbol{F}}}$ and $II_{\hat{\boldsymbol{H}}}$ can be expressed as

$$II_{\hat{\boldsymbol{F}}} = J^{-2/3} II_{\boldsymbol{F}}; \qquad II_{\hat{\boldsymbol{H}}} = J^{-4/3} II_{\boldsymbol{H}} \tag{40}$$

Furthermore, the choice of $3/2$ in the exponent associated with $II_{\hat{H}}$ is motivated by the polyconvexity condition: although $II_{\boldsymbol{H}}$ is polyconvex, its isochoric counterpart, namely $II_{\bar{\boldsymbol{H}}}$ is not polyconvex [**?**]. In fact, $II^{\alpha}_{\bar{\boldsymbol{H}}}$ is polyconvex provided that $\alpha \geq 3/2$, hence the value chosen.

A slightly more complex expression for the strain energy density $\hat{e}_R(\boldsymbol{F}, \boldsymbol{D}_0)$ involving as well the field $\boldsymbol{d}$ is

$$\hat{e}_R(\boldsymbol{F}, \boldsymbol{D}_0) = \hat{\mathbb{W}}_R(\boldsymbol{F}, \boldsymbol{H}, J\boldsymbol{D}_0, \boldsymbol{d}) = \frac{\mu_1}{2} II_{\hat{\boldsymbol{F}}} + \frac{\mu_2}{2} II^{3/2}_{\hat{\boldsymbol{H}}} + \frac{1}{2\varepsilon_1} II_{\boldsymbol{D}_0} + \frac{1}{2\varepsilon_2} II_{\boldsymbol{d}} \tag{41}$$

Use of the Legendre transformation in (35) permits to obtain its free energy density counterpart, namely $\hat{\Psi}_R(\boldsymbol{F}, \boldsymbol{E}_0)$ as

$$\hat{\Psi}_R(\boldsymbol{F}, \boldsymbol{E}_0) = \frac{\mu_1}{2} II_{\hat{\boldsymbol{F}}} + \frac{\mu_2}{2} II^{3/2}_{\hat{\boldsymbol{H}}} - \frac{1}{2\varepsilon_2 J} II_{\boldsymbol{H}\boldsymbol{E}_0} \tag{42}$$

with $II_{\boldsymbol{H}\boldsymbol{E}_0} = \boldsymbol{H}\boldsymbol{E}_0 \cdot \boldsymbol{H}\boldsymbol{E}_0$.

Furthermore, a possible sufficient condition that complies with the two rank-one convexity conditions in equation (34b) for the volumetric terms $\bar{\Psi}_R(J)$ and $\bar{\eta}_R(J)$ is their polyconvexity, which in this case, reduces to their convexity with respect to J. It can clearly be seen that the expression for $\bar{\eta}_R(J)$ in (**??**) is indeed convex with respect to J, i.e. its second derivative with respect to J vanishes. A possible expression for $\bar{\Psi}_R(J)$ can be

$$\bar{\Psi}_R(J) = \frac{\lambda}{2}(J-1)^2; \qquad \lambda > 0 \tag{43}$$

Notice from (**??**) that among the two last conditions in (34), $\bar{g}(\theta) > 0$ is not satisfied. However, we will see that this condition is indeed very restrictive.

The Third Law of thermodynamics: The Third Law of thermodynamics establishes that "the entropy of a body should be zero at Kelvin state (zero temperature)" XXXX, namely

$$\lim_{\theta \to 0} \eta = 0 \tag{44}$$

In addition, the specific heat coefficient, denoted as c_v and defined as

$$c_v\left(\boldsymbol{F}, \boldsymbol{E}_0, \theta, \boldsymbol{\mathcal{A}}\right) = -\theta \partial^2_{\theta^2} \Psi\left(\boldsymbol{F}, \boldsymbol{E}_0, \theta, \boldsymbol{\mathcal{A}}\right), \tag{45}$$

must satisfy the following conditions

$$c_v\left(\boldsymbol{F}, \boldsymbol{E}_0, \theta, \boldsymbol{\mathcal{A}}\right) > 0; \qquad c_v\left(\boldsymbol{I}, \boldsymbol{0}, \theta_R, \boldsymbol{\mathcal{A}}|_{\boldsymbol{I},\boldsymbol{0},\theta_R}\right) = c_v^0 \tag{46}$$

where $c_v^0 \in \mathbb{R}^+$ is the specific heat coefficient at the reference unstressed configuration. Notice that the first condition above can be satisfied provided that the free energy density Ψ is concave with respect to θ, namely

$$\partial^2_{\theta\theta} \Psi < 0. \tag{47}$$

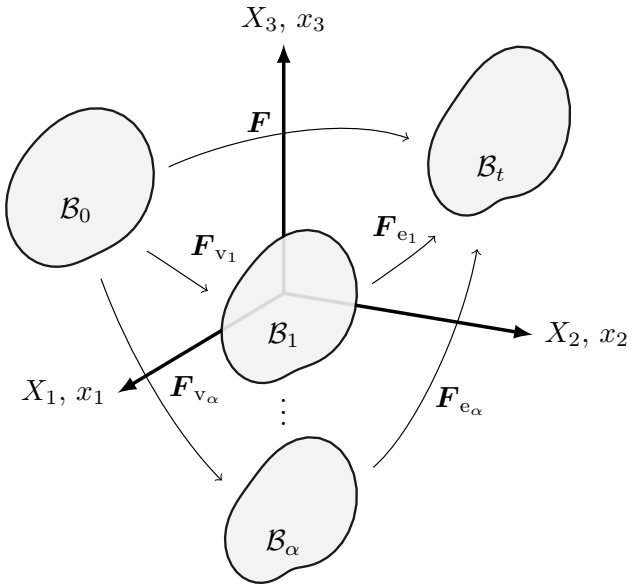

Figure 2: Multiplicative decomposition of the deformation gradient.

Clearly, this is incompatible with the choice of a constant specific heat coefficient c_v as shown by equation XX,

Material frame indifference:

$$\widetilde{\Psi}(\boldsymbol{C}, \boldsymbol{E}_0, \theta, \boldsymbol{\mathcal{A}}) = \Psi(\boldsymbol{F}, \boldsymbol{E}_0, \theta, \boldsymbol{\mathcal{A}}) \tag{48}$$

$$\widetilde{\Psi}(\boldsymbol{C}, \boldsymbol{E}_0, \theta, \boldsymbol{\mathcal{A}}) = \bar{\Psi}_R(\det\boldsymbol{C}) - \bar{g}(\theta)\theta_R\Big(\alpha(J-1) + \frac{c_v^0}{\bar{\gamma}}\Big) + \Big(1 + \hat{g}(\theta)\Big)\hat{\Psi}_R(\boldsymbol{C}, \boldsymbol{E}_0, \boldsymbol{\mathcal{A}}) \tag{49}$$

3.5. Incompressible viscoelasticity at finite strains

This Section presents a theoretical framework for large strain compressible viscoelasticity, where the viscous deformation is not assumed isochoric af a first instance.

3.5.1. Continuum kinematics and multiplicative decomposition

Viscoelasticity in finite strains using a generlized three dimensional Maxwell model is typically formulated using a multiplicative decomposition of the deformation gradient tensor $\boldsymbol{F}$ in terms of its elastic and viscous components [2, 7, 35, 36]

$$\boldsymbol{F} = \boldsymbol{F}_{\mathrm{e}_\alpha}\boldsymbol{F}_{\mathrm{v}_\alpha}, \tag{50}$$

through the introduction of suitable intermediate (i.e. stress free) configurations (see Fig. 2). As it is illustrated, the number of viscous elements $\alpha = 1 \ldots n_\alpha$ in this generalised Maxwell model can be arbitrary. Note that $\boldsymbol{F}_{\mathrm{v}_\alpha}$ denotes the internal variable of the corresponding viscous element α that determines the current state of the system, with thermo-dynamical equilibrium achieved when $\boldsymbol{F}_{\mathrm{v}_\alpha} = \boldsymbol{F}$. Moreover, to ensure that the proposed constitutive model is objective (i.e. frame invariant), suitable rotation free right Cauchy-Green deformation tensors can be defined as

$$\boldsymbol{C} = \boldsymbol{F}^{\mathrm{T}}\boldsymbol{F}; \tag{51a}$$

$$\boldsymbol{C}_{\mathrm{v}_\alpha} = \boldsymbol{F}_{\mathrm{v}_\alpha}^{\mathrm{T}}\boldsymbol{F}_{\mathrm{v}_\alpha}, \tag{51b}$$

where $\boldsymbol{C}$ and $\boldsymbol{C}_{\mathrm{v}_\alpha}$ denote the total and viscous right Cauchy-Green deformation tensors, respectively. It should be pointed out that unlike $\boldsymbol{C}$ and $\boldsymbol{C}_{\mathrm{v}_\alpha}$, the right Cauchy-Green deformation tensor $\boldsymbol{C}_{\mathrm{e}_\alpha} = \boldsymbol{F}_{\mathrm{e}_\alpha}^{\mathrm{T}} \boldsymbol{F}_{\mathrm{e}_\alpha}$ is not defined in the reference configuration, but at the intermediate (elastic free) configuration and, as such, it is not rotation free. Indeed, the multiplicative decomposition of the deformation gradient (50) has an internal redundant rotation, which means $\boldsymbol{F}$ can equally be written as

$$\boldsymbol{F} = \boldsymbol{F}_{\mathrm{e}_\alpha}^{*} \boldsymbol{F}_{\mathrm{v}_\alpha}^{*} \quad \text{with} \quad \boldsymbol{F}_{\mathrm{v}_\alpha}^{*} = \boldsymbol{Q} \boldsymbol{F}_{\mathrm{v}_\alpha} \quad \text{and} \quad \boldsymbol{F}_{\mathrm{e}_\alpha}^{*} = \boldsymbol{F}_{\mathrm{e}_\alpha} \boldsymbol{Q}^{\mathrm{T}}, \tag{52}$$

where $\boldsymbol{Q} \in \mathrm{SO}(3)$ denotes an arbitrary rotation tensor. Following a similar idea to that of Reference [30],5 in this paper we propose to eliminate this redundant rotation by selecting $\boldsymbol{Q}$ as $\boldsymbol{R}_{\mathrm{v}_\alpha}^{\mathrm{T}}$, namely, the rotation tensor emanating from the right polar decomposition of the viscous deformation gradient tensor $\boldsymbol{F}_{\mathrm{v}_\alpha} = \boldsymbol{R}_{\mathrm{v}_\alpha} \boldsymbol{U}_{\mathrm{v}_\alpha}$. Hence, a unique multiplicative decomposition of the deformation gradient $\boldsymbol{F}$ can then be obtained as

$$\boldsymbol{F} = \boldsymbol{F}_{\mathrm{e}_\alpha}^{*} \boldsymbol{U}_{\mathrm{v}_\alpha}, \quad \boldsymbol{F}_{\mathrm{e}_\alpha}^{*} = \boldsymbol{F}_{\mathrm{e}_\alpha} \boldsymbol{R}_{\mathrm{v}_\alpha}, \tag{53}$$

whereby

$$\boldsymbol{C}_{\mathrm{e}_\alpha} = \boldsymbol{F}_{\mathrm{e}_\alpha}^{*\mathrm{T}} \boldsymbol{F}_{\mathrm{e}_\alpha}^{*} = \boldsymbol{U}_{\mathrm{v}_\alpha}^{-1} \boldsymbol{C} \boldsymbol{U}_{\mathrm{v}_\alpha}^{-1}, \tag{54}$$

and the symmetric viscous strain tensor $\boldsymbol{U}_{\mathrm{v}_\alpha}$ is also uniquely defined.

3.6. Strain energy function

To guarantee that Ψ_α vanishes when $\boldsymbol{U}_{\mathrm{v}_\alpha}$ and $\boldsymbol{F}$ only differ by a rigid body rotation (i.e. thermo-dynamical equilibrium), Bonet et al. XXX particularise the definition of Ψ_α as

$$\Psi_\alpha \left(\boldsymbol{C},\ \boldsymbol{U}_{\mathrm{v}_\alpha} \right) = \tilde{\Psi}_\alpha \left(\boldsymbol{C}_{\mathrm{e}_\alpha} \right), \tag{55}$$

where $\boldsymbol{C}_{\mathrm{e}_\alpha}$ is defined in (54) and the symbol $\tilde{\Psi}$ is used to emphasise the alternative functional dependency. Moreover, for the particular case of isotropic viscoelasticity, the strain energy contributions $\Psi_\infty(\boldsymbol{C})$ and $\tilde{\Psi}_\alpha(\boldsymbol{C}_{\mathrm{e}_\alpha})$ can be particularised in terms of their respective invariants $\{I_\bullet, II_\bullet, III_\bullet\}$, which will be implicitly assumed in what follows. Note that extension to the anisotropic case would imply the incorporation of structural tensors representative of their appropriate symmetry groups as further arguments of the strain energy density, which will be presented in a subsequent section.

Incompressibility of the viscous stretch contribution $\boldsymbol{U}_{\mathrm{v}_\alpha}$ implies that $\det \boldsymbol{U}_{\mathrm{v}_\alpha} = 1$ or, alternatively, by recalling (50), that

$$J_{\mathrm{e}_\alpha} = \det \boldsymbol{F}_{\mathrm{e}_\alpha} = \det \boldsymbol{F} = J. \tag{56}$$

Time differentiation of above kinematic constraint (56) leads to

$$\boldsymbol{C}_{\mathrm{e}_\alpha}^{-1} : \left. \frac{\mathrm{d} \boldsymbol{C}_{\mathrm{e}_\alpha}}{\mathrm{d}t} \right|_{\boldsymbol{F}=\mathrm{const}} = 0, \tag{57}$$

which arises as a kinematic constraint for the time evolution of the elastic right Cauchy-Green tensor $\boldsymbol{C}_{\mathrm{e}_\alpha}$. Correspondingly, the Maxwell strain energy density Ψ_α must be defined to only penalise distortional contributions, that is

$$\Psi_\alpha(\boldsymbol{C},\ \boldsymbol{U}_{\mathrm{v}_\alpha}) = \hat{\tilde{\Psi}}_\alpha \left(\boldsymbol{C}_{\mathrm{e}_\alpha} \right) = \tilde{\Psi}_\alpha \left(\hat{\boldsymbol{C}}_{\mathrm{e}_\alpha} \right); \qquad \hat{\boldsymbol{C}}_{\mathrm{e}_\alpha} = J_{\mathrm{e}_\alpha}^{-\frac{2}{3}} \boldsymbol{C}_{\mathrm{e}_\alpha}, \tag{58}$$

whereby[5] the (deviatoric) second Piola-Kirchhoff elastic stress $\boldsymbol{S}'_{\mathrm{e}_\alpha} = 2\frac{\partial \hat{\tilde{\Psi}}_\alpha(\boldsymbol{C}_{\mathrm{e}_\alpha})}{\partial \boldsymbol{C}_{\mathrm{e}_\alpha}}$ can be shown to verify[6]

$$\boldsymbol{S}'_{\mathrm{e}_\alpha} : \boldsymbol{C}_{\mathrm{e}_\alpha} = 0, \tag{59}$$

which can be understood as an alternative kinetic (i.e. stress based) constraint to those of (56) or (57) to fulfil incompressibility[7]. Further differentiation of this constraint and application of (57) results in an alternative incompressibility constraint

$$\boldsymbol{C}_{\mathrm{e}_\alpha} : \mathbb{C}_{\mathrm{e}_\alpha} : \boldsymbol{C}_{\mathrm{e}_\alpha} = 0, \tag{60}$$

in terms of the fourth order elasticity tensor $\mathbb{C}_{\mathrm{e}_\alpha}$ [8]. Note that, due to its deviatoric nature, $\mathbb{C}_{\mathrm{e}_\alpha}$ is not strictly positive definite (refer to (60)) and cannot thus be directly inverted, so the evolution law in (67) needs to be suitably adapted, which will be presented in the following section.

3.7. Second Piola-Kirchhoff stress tensor

The second Piola-Kirchhoff stress tensor $\boldsymbol{S}$ can now be obtained from the directional derivative of the strain energy Ψ with respect to a perturbation $\delta\boldsymbol{C}$ whilst holding the internal state variable $\boldsymbol{U}_{\mathrm{v}_\alpha}$ constant (i.e. $D\,\Psi|_{\boldsymbol{U}_{\mathrm{v}_\alpha}=\mathrm{const}}[\delta\boldsymbol{C}] = \boldsymbol{S} : \frac{1}{2}\delta\boldsymbol{C}$), to yield

$$\boldsymbol{S} = 2\frac{\partial \Psi}{\partial \boldsymbol{C}} = \boldsymbol{S}_\infty + \sum_\alpha \boldsymbol{S}_\alpha, \quad \boldsymbol{S}_\infty = 2\frac{\partial \Psi_\infty}{\partial \boldsymbol{C}}, \quad \boldsymbol{S}_\alpha = 2\left.\frac{\partial \Psi_\alpha}{\partial \boldsymbol{C}}\right|_{\boldsymbol{U}_{\mathrm{v}_\alpha}=\mathrm{const}}, \tag{61}$$

where $\boldsymbol{S}_\infty$ represents the long-term stress tensor and $\boldsymbol{S}_\alpha$ denotes the viscous stress tensor of the corresponding Maxwell element and the symbol $(\bullet)|_{\boldsymbol{U}_{\mathrm{v}_\alpha}=\mathrm{const}}$ emphasises that the internal state variable $\boldsymbol{U}_{\mathrm{v}_\alpha}$ is held constant. Note that from (55) and the definition (54), stress $\boldsymbol{S}_\alpha$ will vanish when $\boldsymbol{U}_{\mathrm{v}_\alpha}$ only differs from $\boldsymbol{F}$ by a rigid body rotation. For the subsequent derivation, the elastic second Piola-Kirchhoff stress tensor of the viscous Maxwell element $\boldsymbol{S}_{\mathrm{e}_\alpha}$ is defined as

$$\boldsymbol{S}_{\mathrm{e}_\alpha} = 2\frac{\partial \tilde{\Psi}_\alpha\left(\boldsymbol{C}_{\mathrm{e}_\alpha}\right)}{\partial \boldsymbol{C}_{\mathrm{e}_\alpha}}. \tag{62}$$

It is now useful to relate stress $\boldsymbol{S}_\alpha$ $(61)_c$ to stress $\boldsymbol{S}_{\mathrm{e}_\alpha}$ (62) by noticing that

$$D\,\Psi_\alpha|_{\boldsymbol{U}_{\mathrm{v}_\alpha}=\mathrm{const}}[\delta\boldsymbol{C}] = D\tilde{\Psi}_\alpha[D\,\boldsymbol{C}_{\mathrm{e}_\alpha}|_{\boldsymbol{U}_{\mathrm{v}_\alpha}=\mathrm{const}}[\delta\boldsymbol{C}]], \tag{63}$$

and substituting the directional derivative of (54) with respect to $\delta\boldsymbol{C}$ into (63) results in

$$\boldsymbol{S}_{\mathrm{e}_\alpha} = \boldsymbol{U}_{\mathrm{v}_\alpha}\boldsymbol{S}_\alpha\boldsymbol{U}_{\mathrm{v}_\alpha}, \tag{64}$$

which establishes a necessary relationship between the Maxwell viscous contribution to the second Piola-Kirchhoff stress tensor and its elastic counterpart.

---

[5] For the particular isotropic case, the strain energy $\tilde{\Psi}_\alpha$ depends on $\hat{\boldsymbol{C}}_{\mathrm{e}_\alpha}$ via its first two invariants $\{I_\bullet, II_\bullet\}$.

[6] As standard, the deviatoric nature of the stress tensor is emphasised using the superscript $'$ symbol.

[7] This kinetic constraint results from the homogeneous nature of order 0 of the Maxwell strain energy function $\hat{\tilde{\Psi}}_\alpha$, that is, $\hat{\tilde{\Psi}}_\alpha(\boldsymbol{C}_{\mathrm{e}_\alpha}) = \hat{\tilde{\Psi}}_\alpha(\alpha\boldsymbol{C}_{\mathrm{e}_\alpha})$, for any arbitrary constant α [15].

[8] Constraints (59) and (60) can be easily obtained by computing first and second derivatives of $\hat{\tilde{\Psi}}_\alpha(\alpha\boldsymbol{C}_{\mathrm{e}_\alpha})$ with respect to α, evaluated at $\alpha = 1$.

3.8. Viscous dissipation and evolution law

To fully determine the proposed viscoelastic model, an evolution law for the set of internal variables $\boldsymbol{U}_{\mathrm{v}_\alpha}(\alpha = 1 \dots n_\alpha)$ must be defined. Reference [11] introduces an evolution law based on the relaxation form of the viscous stress, that is, a natural extension of (**??**) to the three dimensional continua. This is accomplished by simply replacing the one-dimensional force and displacement in (**??**) with second Piola-Kirchhoff and right Cauchy-Green tensor counterparts, respectively. However, the non-satisfaction of *ab initio* positive viscous dissipation in [11] (i.e. Coleman-Noll procedure [29]) motivates the further development of this theory in this work. As such, the rate of energy dissipation due to viscous effects is defined as

$$\begin{aligned}
\mathrm{D}_{\mathrm{vis}} &= -\sum_\alpha \frac{\partial \Psi_\alpha}{\partial \boldsymbol{U}_{\mathrm{v}_\alpha}} : \dot{\boldsymbol{U}}_{\mathrm{v}_\alpha} \\
&= -\sum_\alpha \left. \frac{\mathrm{d}\Psi_\alpha\left(\boldsymbol{C},\ \boldsymbol{U}_{\mathrm{v}_\alpha}\right)}{\mathrm{d}t} \right|_{\boldsymbol{F}=\mathrm{const}} \\
&= -\sum_\alpha \left. \frac{\mathrm{d}\tilde{\Psi}_\alpha\left(\boldsymbol{C}_{\mathrm{e}_\alpha}\left(\boldsymbol{C},\ \boldsymbol{U}_{\mathrm{v}_\alpha}\right)\right)}{\mathrm{d}t} \right|_{\boldsymbol{F}=\mathrm{const}} \\
&= -\sum_\alpha \frac{1}{2}\boldsymbol{S}_{\mathrm{e}_\alpha} : \left. \frac{\mathrm{d}\boldsymbol{C}_{\mathrm{e}_\alpha}\left(\boldsymbol{C},\ \boldsymbol{U}_{\mathrm{v}_\alpha}\right)}{\mathrm{d}t} \right|_{\boldsymbol{F}=\mathrm{const}},
\end{aligned} \tag{65}$$

where the explicit dependence of $\boldsymbol{C}_{\mathrm{e}_\alpha}$ on arguments $\{\boldsymbol{C},\ \boldsymbol{U}_{\mathrm{v}_\alpha}\}$ is displayed. To ensure that the evolution law is compatible with the second law of thermodynamics [29], the condition $\mathrm{D}_{\mathrm{vis}} \geq 0$ must be satisfied regardless of the current state of deformation and stress. In order to achieve this, note firstly that

$$\left. \frac{\mathrm{d}\boldsymbol{C}_{\mathrm{e}_\alpha}}{\mathrm{d}t} \right|_{\boldsymbol{F}=\mathrm{const}} = 2\mathbb{C}_{\mathrm{e}_\alpha}^{-1} : \left. \frac{\mathrm{d}\boldsymbol{S}_{\mathrm{e}_\alpha}}{\mathrm{d}t} \right|_{\boldsymbol{F}=\mathrm{const}}, \tag{66}$$

where $\mathbb{C}_{\mathrm{e}_\alpha} = 2\frac{\partial \boldsymbol{S}_{\mathrm{e}_\alpha}}{\partial \boldsymbol{C}_{\mathrm{e}_\alpha}}$ is the so-called fourth order (positive definite) Lagrangian elasticity tensor. Crucially, $\mathbb{C}_{\mathrm{e}_\alpha}$ and its inverse $\mathbb{C}_{\mathrm{e}_\alpha}^{-1}$ can be straightforwardly obtained for simple user defined strain energy densities (i.e. Saint-Venant, neo-Hookean) [15]. Using Eq. (66), the internal viscous dissipation can now be rewritten as

$$\mathrm{D}_{\mathrm{vis}} = -\sum_\alpha \boldsymbol{S}_{\mathrm{e}_\alpha} : \mathbb{C}_{\mathrm{e}_\alpha}^{-1} : \left. \frac{\mathrm{d}\boldsymbol{S}_{\mathrm{e}_\alpha}}{\mathrm{d}t} \right|_{\boldsymbol{F}=\mathrm{const}}, \tag{67}$$

where in order to ensure positive dissipation, the following general evolution law is proposed

$$\left. \frac{\mathrm{d}\boldsymbol{S}_{\mathrm{e}_\alpha}}{\mathrm{d}t} \right|_{\boldsymbol{F}=\mathrm{const}} = -\frac{1}{\tau_\alpha}\boldsymbol{S}_{\mathrm{e}_\alpha}; \qquad \tau_\alpha > 0, \tag{68}$$

where τ_α represents the relaxation time parameter that determines the rate of dissipation of the viscous stresses. For completeness, by the use of Eq. (68), the viscous dissipation can finally take the form of

$$\mathrm{D}_{\mathrm{vis}} = \sum_\alpha \frac{1}{\tau_\alpha}\boldsymbol{S}_{\mathrm{e}_\alpha} : \mathbb{C}_{\mathrm{e}_\alpha}^{-1} : \boldsymbol{S}_{\mathrm{e}_\alpha} \geq 0. \tag{69}$$

Since the elastic second Piola-Kirchhoff stress tensor $\boldsymbol{S}_{\mathrm{e}_\alpha}$ is a function of both the total deformation gradient $\boldsymbol{F}$ and viscous stretch $\boldsymbol{U}_{\mathrm{v}_\alpha}$, the left-hand side of (68) can be transformed as

$$\left. \frac{\partial \boldsymbol{S}_{\mathrm{e}_\alpha}}{\partial \boldsymbol{U}_{\mathrm{v}_\alpha}} \right|_{\boldsymbol{F}=\mathrm{const}} : \dot{\boldsymbol{U}}_{\mathrm{v}_\alpha} = -\frac{1}{\tau_\alpha}\boldsymbol{S}_{\mathrm{e}_\alpha}, \tag{70}$$

thereby leading to the determination of the state variable $\boldsymbol{U}_{\mathrm{v}_\alpha}$ in the following nonlinear form

$$\dot{\boldsymbol{U}}_{\mathrm{v}_\alpha} = -\frac{1}{\tau_\alpha}\mathbb{M}_{\mathrm{e}_\alpha}^{-1} : \boldsymbol{S}_{\mathrm{e}_\alpha}, \tag{71}$$

where the fourth-order tensor $\mathbb{M}_{\mathrm{e}_\alpha}$ is defined by

$$\mathbb{M}_{\mathrm{e}_\alpha} = \left.\frac{\partial \boldsymbol{S}_{\mathrm{e}_\alpha}}{\partial \boldsymbol{U}_{\mathrm{v}_\alpha}}\right|_{\boldsymbol{F}=\text{const}}. \tag{72}$$

Interestingly, note that Eq. (71) is very similar to the plastic evolution equation in the context of maximum dissipation-based large strain elastoplasticity, as described in [53, 54], facilitating thus the link between both inelastic approaches. It is straightforward to show that Eq. (71) corresponds to the plastic evolution equation in which the non-equilibrium strain energy function is replaced with the yield surface function and the elastic regime has been collapsed to the original state. In this sense, Eq. (68) can be also generalised into the plastic case by simply replacing the right-hand side with an appropriate flow rule. It is important to emphasise that the fourth tensor $\mathbb{M}_{\mathrm{e}_\alpha}$ encapsulates a nonlinear dependence on both the strain and the internal state variables.

It should also be pointed out that although the evolution equation (71) for the state variables $\boldsymbol{U}_{\mathrm{v}_\alpha}$ is nonlinear, the relaxation law embodied by Eq. (68) is generally linear (similar to the idea pursued in [52]) except when the parameter τ_α is also a function of the stresses. Note that the only requirement to ensure positive dissipation is that τ_α is positive, but not necessarily constant, that is, $\tau_\alpha = f(\|\boldsymbol{S}_{\mathrm{e}_\alpha}\|)$, with f a non-negative function. Furthermore, more general fully nonlinear evolution laws can be developed using the concept of a dissipation potential as described in the Remark below.

A straightforward way to guarantee the invertibility of the singular fourth order elasticity tensor $\mathbb{C}_{\mathrm{e}_\alpha}$ can be obtained via the following additive extension

$$\bar{\mathbb{C}}_{\mathrm{e}_\alpha} = 2\frac{\partial \boldsymbol{S}'_{\mathrm{e}_\alpha}}{\partial \boldsymbol{C}_{\mathrm{e}_\alpha}} + m\boldsymbol{C}_{\mathrm{e}_\alpha}^{-1} \otimes \boldsymbol{C}_{\mathrm{e}_\alpha}^{-1}, \tag{73}$$

where m denotes an arbitrary positive constant adopting the role of an artificial bulk modulus which guarantees the positive definiteness of the newly defined enhanced elasticity tensor $\bar{\mathbb{C}}_{\mathrm{e}_\alpha}$. It is clear now that application of (60) into $\bar{\mathbb{C}}_{\mathrm{e}_\alpha}$ renders $9m > 0$. As a result, Eq. (66) is re-defined as

$$\left.\frac{\mathrm{d}\boldsymbol{C}_{\mathrm{e}_\alpha}}{\mathrm{d}t}\right|_{\boldsymbol{F}=\text{const}} = 2\bar{\mathbb{C}}_{\mathrm{e}_\alpha}^{-1} : \left.\frac{\mathrm{d}\boldsymbol{S}'_{\mathrm{e}_\alpha}}{\mathrm{d}t}\right|_{\boldsymbol{F}=\text{const}}. \tag{74}$$

The evolution law for $\boldsymbol{S}'_{\mathrm{e}_\alpha}$ embodied by Eq. (68) in the compressible case, can now be adjusted in order to comply with the incompressibility constraint Eq. (57). This can be carried out via the use of a scalar parameter λ_α (i.e. Lagrange multiplier) to give

$$\left.\frac{\mathrm{d}\boldsymbol{S}'_{\mathrm{e}_\alpha}}{\mathrm{d}t}\right|_{\boldsymbol{F}=\text{const}} = -\frac{1}{\tau_\alpha}\left(\boldsymbol{S}'_{\mathrm{e}_\alpha} - \lambda_\alpha \boldsymbol{C}_{\mathrm{e}_\alpha}^{-1}\right), \tag{75}$$

where the last term on the right hand side represent a possible volumetric stress contribution. Using Eqs. (57) and (74) along with above Eq. (75), the value of λ_α can be obtained after simple algebra as

$$\lambda_\alpha = \frac{\boldsymbol{S}'_{\mathrm{e}_\alpha} : \bar{\mathbb{C}}_{\mathrm{e}_\alpha}^{-1} : \boldsymbol{C}_{\mathrm{e}_\alpha}^{-1}}{\boldsymbol{C}_{\mathrm{e}_\alpha}^{-1} : \bar{\mathbb{C}}_{\mathrm{e}_\alpha}^{-1} : \boldsymbol{C}_{\mathrm{e}_\alpha}^{-1}}, \tag{76}$$

from where the positive dissipation Eq. (67) now becomes

$$\begin{aligned}
\mathrm{D}_{\mathrm{vis}} &= -\sum_{\alpha} \boldsymbol{S}'_{\mathrm{e}_\alpha} : \bar{\mathbb{C}}^{-1}_{\mathrm{e}_\alpha} : \left.\frac{\mathrm{d}\boldsymbol{S}'_{\mathrm{e}_\alpha}}{\mathrm{d}t}\right|_{\boldsymbol{F}=\mathrm{const}} \\
&= \sum_{\alpha} \frac{1}{\tau_\alpha} \boldsymbol{S}'_{\mathrm{e}_\alpha} : \bar{\mathbb{C}}^{-1}_{\mathrm{e}_\alpha} : \left(\boldsymbol{S}'_{\mathrm{e}_\alpha} - \frac{\boldsymbol{S}'_{\mathrm{e}_\alpha} : \bar{\mathbb{C}}^{-1}_{\mathrm{e}_\alpha} : \boldsymbol{C}^{-1}_{\mathrm{e}_\alpha}}{\boldsymbol{C}^{-1}_{\mathrm{e}_\alpha} : \bar{\mathbb{C}}^{-1}_{\mathrm{e}_\alpha} : \boldsymbol{C}^{-1}_{\mathrm{e}_\alpha}} \boldsymbol{C}^{-1}_{\mathrm{e}_\alpha} \right) \\
&= \sum_{\alpha} \frac{1}{\tau_\alpha} \frac{(\boldsymbol{S}'_{\mathrm{e}_\alpha} : \bar{\mathbb{C}}^{-1}_{\mathrm{e}_\alpha} : \boldsymbol{S}'_{\mathrm{e}_\alpha})(\boldsymbol{C}^{-1}_{\mathrm{e}_\alpha} : \bar{\mathbb{C}}^{-1}_{\mathrm{e}_\alpha} : \boldsymbol{C}^{-1}_{\mathrm{e}_\alpha}) - (\boldsymbol{S}'_{\mathrm{e}_\alpha} : \bar{\mathbb{C}}^{-1}_{\mathrm{e}_\alpha} : \boldsymbol{C}^{-1}_{\mathrm{e}_\alpha})^2}{\boldsymbol{C}^{-1}_{\mathrm{e}_\alpha} : \bar{\mathbb{C}}^{-1}_{\mathrm{e}_\alpha} : \boldsymbol{C}^{-1}_{\mathrm{e}_\alpha}} \\
&\geq 0,
\end{aligned} \tag{77}$$

and the positive value of the numerator is a consequence of the Cauchy-Schwarz inequality. An alternative derivation of the evolution law (75) and the value of the Lagrange multiplier (76) can be found in Appendix **??**.

3.9. Incremental evolution law

For the sake of computational implementation, Eq. (71) would need to be integrated in time so as to update the state variables $\boldsymbol{U}_{\mathrm{v}_\alpha}$ from time step n to time step $n+1$. However, the direct use of this equation is highly cumbersome, and thus it is preferable to transform the left-hand side of Eq. (68) into an incremental form, which when using a classical (first order) backward Euler scheme renders

$$\left.\frac{\mathrm{d}\boldsymbol{S}_{\mathrm{e}_\alpha}}{\mathrm{d}t}\right|_{\boldsymbol{F}=\mathrm{const}} = \frac{1}{\Delta t}\left(\boldsymbol{S}^{n+1}_{\mathrm{e}_\alpha} - \boldsymbol{S}^{*}_{\mathrm{e}_\alpha}\right), \tag{78}$$

where Δt denotes the time step size, and the stress tensors $\boldsymbol{S}^{n+1}_{\mathrm{e}_\alpha}$ and $\boldsymbol{S}^{*}_{\mathrm{e}_\alpha}$ are defined by

$$\boldsymbol{S}^{*}_{\mathrm{e}_\alpha} = \boldsymbol{S}_{\mathrm{e}_\alpha}\left(\boldsymbol{C}^{n+1},\, \boldsymbol{U}^{n}_{\mathrm{v}_\alpha}\right) \quad \text{and} \quad \boldsymbol{S}^{n+1}_{\mathrm{e}_\alpha} = \boldsymbol{S}_{\mathrm{e}_\alpha}\left(\boldsymbol{C}^{n+1},\, \boldsymbol{U}^{n+1}_{\mathrm{v}_\alpha}\right), \tag{79}$$

where the upper script n and $n+1$ indicate evaluation in their corresponding time steps. Note that $\boldsymbol{S}^{*}_{\mathrm{e}_\alpha}$ represents the state of stress attained from the assumption that there is no viscous deformation taking place from time step n to $n+1$. Alternatively, it can also be interpreted as the state of stress attained when the deformation from time step n to $n+1$ takes place instantaneously[9]. In the context of viscoelasticity, the stress relaxation is inevitable and the final stress can be derived by substituting (78) into (68), resulting in

$$\frac{1}{\Delta t}\left(\boldsymbol{S}^{n+1}_{\mathrm{e}_\alpha} - \boldsymbol{S}^{*}_{\mathrm{e}_\alpha}\right) = -\frac{1}{\tau_\alpha}\boldsymbol{S}^{n+1}_{\mathrm{e}_\alpha}, \tag{80}$$

which after simple rearrangement results in

$$\boldsymbol{S}^{n+1}_{\mathrm{e}_\alpha} = \gamma_\alpha \boldsymbol{S}^{*}_{\mathrm{e}_\alpha}; \qquad \gamma_\alpha = \frac{\tau_\alpha}{\tau_\alpha + \Delta t}. \tag{81}$$

Note that the final relaxation stress $\boldsymbol{S}^{n+1}_{\mathrm{e}_\alpha}$ is proportional to the instantaneous stress $\boldsymbol{S}^{*}_{\mathrm{e}_\alpha}$ [10], and compared with the direct time integration of Eqs. (71)-(72), computational implementation of

[9] In the case of elastoplasticity, this term is known as the trial stress that may or may not satisfy the yield inequality.

[10] This projection can be identified with the radial return scheme in the context of elastoplasticity

(81) is considerably simpler. Once the final relaxation stress $\boldsymbol{S}_{\mathrm{e}_\alpha}^{n+1}$ is computed, the elastic right-Cauchy-Green strain tensor $\boldsymbol{C}_{\mathrm{e}_\alpha}^{n+1}$ can be determined making use of the user-defined strain energy density $\tilde{\Psi}_\alpha$. After obtaining $\boldsymbol{C}_{\mathrm{e}_\alpha}^{n+1}$, the corresponding viscous state variable $\boldsymbol{U}_{\mathrm{v}_\alpha}^{n+1}$ can be derived from (54). It is possible to show by direct substitution that the symmetric viscous stretch tensor $\boldsymbol{U}_{\mathrm{v}_\alpha}^{n+1}$ can be obtained as

$$\boldsymbol{U}_{\mathrm{v}_\alpha}^{n+1} = \left(\boldsymbol{U}_{\mathrm{e}_\alpha}^{n+1}\right)^{-1} \left(\boldsymbol{U}_{\mathrm{e}_\alpha}^{n+1}\boldsymbol{C}^{n+1}\boldsymbol{U}_{\mathrm{e}_\alpha}^{n+1}\right)^{\frac{1}{2}} \left(\boldsymbol{U}_{\mathrm{e}_\alpha}^{n+1}\right)^{-1}; \qquad \boldsymbol{U}_{\mathrm{e}_\alpha}^{n+1} = \left(\boldsymbol{C}_{\mathrm{e}_\alpha}^{n+1}\right)^{\frac{1}{2}}. \tag{82}$$

The numerical procedure for the calculation of the internal variable $\boldsymbol{U}_{\mathrm{v}_\alpha}^{n+1}$ is outlined in Algorithm 1.

Algorithm 1 Numerical procedure for the calculation of the internal variable in the compressible case.

for *Time Increment* $= 1, 2, \ldots$ **do**
  for *Iteration* $= 1, 2, \ldots$ **do**
    Calculate the right Cauchy-Green strain tensor at the current time increment $\boldsymbol{C}^{n+1}$
    Compute the instantaneous stress tensor $\boldsymbol{S}_{\mathrm{e}_\alpha}^{*}$
    Compute the stress relaxation $\boldsymbol{S}_{\mathrm{e}_\alpha}^{n+1}$ via Eq. (81)
    Obtain the elastic right Cauchy-Green tensor $\boldsymbol{C}_{\mathrm{e}_\alpha}^{n+1}$ via stress energy density $\tilde{\Psi}_\alpha$
    Determine the internal variable $\boldsymbol{U}_{\mathrm{v}_\alpha}^{n+1}$ according to Eq. (82)
  end for
  Store the internal variable $\boldsymbol{U}_{\mathrm{v}_\alpha}^{n+1}$ as history variable
end for

Notice that for the case of a simple Saint–Venant–Kirchhoff material model, computation of $\boldsymbol{C}_{\mathrm{e}_\alpha}^{n+1}$ accepts a closed-form solution, whilst for other more nonlinear models (i.e. neo-Hookean), a simple Newton-Raphson scheme can be needed. Specifically, in the case of the simple Saint–Venant–Kirchhoff material model, (81) results in

$$\frac{1}{2}\lambda_\alpha \left(\mathrm{tr}\boldsymbol{C}_{\mathrm{e}_\alpha}^{n+1} - 3\right)\boldsymbol{I} + \mu_\alpha\left(\boldsymbol{C}_{\mathrm{e}_\alpha}^{n+1} - \boldsymbol{I}\right) = \gamma_\alpha \boldsymbol{S}_{\mathrm{e}_\alpha}^{*}, \tag{83}$$

expressed in terms of the lame coefficients λ_α and μ_α, which admits a closed-form solution for $\boldsymbol{C}_{\mathrm{e}_\alpha}^{n+1}$. Analogously, in the case of a neo-Hookean material model, (81) takes the explicit form of

$$\mu_\alpha\left(\boldsymbol{I} - \left(\boldsymbol{C}_{\mathrm{e}_\alpha}^{n+1}\right)^{-1}\right) + \frac{\lambda_\alpha}{2}\ln\left({}^{\mathrm{det}}\boldsymbol{C}_{\mathrm{e}_\alpha}^{n+1}\right)\left(\boldsymbol{C}_{\mathrm{e}_\alpha}^{n+1}\right)^{-1} = \gamma_\alpha \boldsymbol{S}_{\mathrm{e}_\alpha}^{*}, \tag{84}$$

which can be easily solved for $\boldsymbol{C}_{\mathrm{e}_\alpha}^{n+1}$ via a Newton-Raphson type of iterative solution scheme.

Incompressibility

Following a similar procedure to that described in Section 3.9, Eq. (75) can be integrated in time (i.e. first order backward Euler) as

$$\frac{1}{\Delta t}(\boldsymbol{S}'^{n+1}_{\mathrm{e}_\alpha} - \boldsymbol{S}'^{*}_{\mathrm{e}_\alpha}) = -\frac{1}{\tau_\alpha}\left(\boldsymbol{S}'^{n+1}_{\mathrm{e}_\alpha} - \lambda_\alpha^{n+1}\left(\boldsymbol{C}_{\mathrm{e}_\alpha}^{n+1}\right)^{-1}\right), \tag{85}$$

where $\boldsymbol{S}'^{*}_{\mathrm{e}_\alpha}$ and $\boldsymbol{S}'^{n+1}_{\mathrm{e}_\alpha}$ are defined as

$$\boldsymbol{S}'^{*}_{\mathrm{e}_\alpha} = \boldsymbol{S}'_{\mathrm{e}_\alpha}\left(\boldsymbol{C}^{n+1},\ \boldsymbol{U}_{\mathrm{v}_\alpha}^{n}\right) \quad \text{and} \quad \boldsymbol{S}'^{n+1}_{\mathrm{e}_\alpha} = \boldsymbol{S}'_{\mathrm{e}_\alpha}\left(\boldsymbol{C}^{n+1},\ \boldsymbol{U}_{\mathrm{v}_\alpha}^{n+1}\right), \tag{86}$$

and λ_α^{n+1} can be incrementally obtained by enforcing the constraint

$$\det \boldsymbol{C}_{\mathrm{e}_\alpha}^{n+1} = J_{n+1}^2, \tag{87}$$

rather than using Eq. (76), which only enforces the rate form of the incompressibility constraint[11]. Notably, Eqs. (85) and (87) represent an implicit system of nonlinear equations for the solution of $\boldsymbol{U}_{\mathrm{v}_\alpha}^{n+1}$ and λ_α^{n+1} in terms of $\mathbf{C}^{n+1}$ and $\boldsymbol{U}_{\mathrm{v}_\alpha}^{n}$. Its solution process can be broken-down as previously done in Section 3.9. Specifically, provided $\mathbf{C}^{n+1}$ and $\boldsymbol{U}_{\mathrm{v}_\alpha}^{n}$, Eqs. (85) and (87) can be first solved in terms of $\boldsymbol{C}_{\mathrm{e}_\alpha}^{n+1}$ and λ_α^{n+1} prior definition of the trial stress tensor $\boldsymbol{S}_{\mathrm{e}_\alpha}^{\prime *}$ and with knowledge of the Maxwell viscous strain energy density $\hat{\tilde{\Psi}}_\alpha$. Subsequently, the viscous stretch tensor $\boldsymbol{U}_{\mathrm{v}_\alpha}^{n+1}$ can be evaluated by using Eq. (82). The numerical procedure for the calculation of the internal variable $\boldsymbol{U}_{\mathrm{v}_\alpha}^{n+1}$ is outlined in Algorithm 2.

Algorithm 2 Numerical procedure for the calculation of the internal variable in the incompressible case.

1: **for** *Time Increment* $= 1, 2, \ldots$ **do**
2: **for** *Iteration* $= 1, 2, \ldots$ **do**
3: Calculate the right Cauchy-Green strain tensor at the current time increment $\boldsymbol{C}^{n+1}$
4: Compute the instantaneous stress tensor $\boldsymbol{S}_{\mathrm{e}_\alpha}^{\prime *}$
5: Obtain the elastic right Cauchy-Green tensor $\boldsymbol{C}_{\mathrm{e}_\alpha}^{n+1}$ by the solution of Eq. (85) and Eq. (87)
6: Determine the internal variable $\boldsymbol{U}_{\mathrm{v}_\alpha}^{n+1}$ according to Eq. (82)
7: **end for**
8: Store the internal variable $\boldsymbol{U}_{\mathrm{v}_\alpha}^{n+1}$ as history variable
9: **end for**

Nonetheless, it is instructive to demonstrate the technique for the selected case of an incompressible viscous strain energy density neo-Hookean model, which can be solved analytically. Firstly, by re-arranging Eq. (85), it yields

$$\boldsymbol{S}_{\mathrm{e}_\alpha}^{\prime n+1} - \bar{\eta}^{n+1} \left(\boldsymbol{C}_{\mathrm{e}_\alpha}^{n+1}\right)^{-1} = \gamma_\alpha \boldsymbol{S}_{\mathrm{e}_\alpha}^{\prime *}; \qquad \bar{\eta}^{n+1} = \frac{\Delta t}{\tau_\alpha + \Delta t} \lambda_\alpha^{n+1}; \qquad \gamma_\alpha = \frac{\tau_\alpha}{\tau_\alpha + \Delta t}. \tag{88}$$

For an incompressible new-Hookean strain energy density, the expression for the second Piola-Kirchhoff stress tensor [15] can be substituted into $(88)_a$ to give

$$\mu_\alpha J_{n+1}^{-\frac{2}{3}} \left(\boldsymbol{I} - \frac{1}{3} \mathrm{tr} \boldsymbol{C}_{\mathrm{e}_\alpha}^{n+1} \left(\boldsymbol{C}_{\mathrm{e}_\alpha}^{n+1}\right)^{-1} \right) - \bar{\eta}^{n+1} \left(\boldsymbol{C}_{\mathrm{e}_\alpha}^{n+1}\right)^{-1} = \gamma_\alpha \boldsymbol{S}_{\mathrm{e}_\alpha}^{\prime *}, \tag{89}$$

where μ_α is the selected shear modulus and, after some simple algebra, above equation (89) can be re-arranged to yield

$$\boldsymbol{C}_{\mathrm{e}_\alpha}^{n+1} = \bar{\gamma}_{n+1} \left(\boldsymbol{I} - \frac{\gamma_\alpha}{\mu_\alpha} J_{n+1}^{\frac{2}{3}} \boldsymbol{S}_{\mathrm{e}_\alpha}^{\prime *} \right)^{-1}, \tag{90}$$

in terms of a yet unknown coefficient $\bar{\gamma}^{n+1}$ formulated as

$$\bar{\gamma}^{n+1} = \frac{\mu_\alpha \mathrm{tr} \boldsymbol{C}_{\mathrm{e}_\alpha}^{n+1} + 3 \bar{\eta}^{n+1} J_{n+1}^{\frac{2}{3}}}{3 \mu_\alpha}. \tag{91}$$

[11] This is similar to classical time integration return mapping approaches in elastoplasticity [53, 54] for the computation of the algorithmic tangent modulus.

In order to determine $\bar{\gamma}^{n+1}$, we can enforce

$$\det \boldsymbol{C}_{\mathrm{e}_\alpha}^{n+1} = \frac{\bar{\gamma}_{n+1}^3}{\det\left(\boldsymbol{I} - \frac{\gamma_\alpha}{\mu_\alpha} J_{n+1}^{\frac{2}{3}} \boldsymbol{S}_{\mathrm{e}_\alpha}^{\prime *}\right)} = J_{n+1}, \tag{92}$$

leading to the explicit evaluation of coefficient $\bar{\gamma}^{n+1}$ as

$$\bar{\gamma}_{n+1} = J_{n+1}^{\frac{2}{3}} \left(\det\left(\boldsymbol{I} - \frac{\gamma_\alpha}{\mu_\alpha} J_{n+1}^{\frac{2}{3}} \boldsymbol{S}_{\mathrm{e}_\alpha}^{\prime *}\right)\right)^{\frac{1}{3}}, \tag{93}$$

which along with (90) provides a computationally efficient closed-form expression for $\boldsymbol{C}_{\mathrm{e}_\alpha}^{n+1}$.

4. Incompressible viscoelasticity at finite strains

In the previous Section, the viscous stretch tensor $\boldsymbol{U}_{\mathrm{v}_\alpha}$ can in general contain both volumetric and distortional components. However, for many viscoelastic materials, the viscous deformation is usually assumed isochoric, and so in this section we will present a modified theory for incompressible viscoelasticity at finite strains.

4.1. Volume-preserving constraints

4.2. Modified viscous dissipation and evolution law

4.3. Incremental equations of the modified evolution law

4.4. Fourier law

Fourier law relates the spatial heat flux $\boldsymbol{q}$ and the spatial gradient of θ by virtue of the following expression

$$\boldsymbol{q} = -\boldsymbol{k}\boldsymbol{\nabla}\theta, \tag{94}$$

where $\boldsymbol{k}$ represents the semi-positive definite second order thermal conductivity tensor in the deformed configuration and $\boldsymbol{\nabla}(\bullet)$ the spatial gradient operator. As customary in continuum mechanics, the relation between $\boldsymbol{q}$ and its material counterpart $\boldsymbol{Q}$ featuring in equation (6) can be carried out by making use of the Gauss' theorem and the Nanson's rule (i.e. $d\boldsymbol{a} = \boldsymbol{H} d\boldsymbol{A}$) as

$$\int_{\mathcal{B}} \mathrm{div}\boldsymbol{q}\, dv = \int_{\partial\mathcal{B}} \boldsymbol{q} \cdot d\boldsymbol{a} = \int_{\partial\mathcal{B}_0} \boldsymbol{Q} \cdot d\boldsymbol{A}, \tag{95}$$

where $\mathrm{div}(\bullet)$ represents the spatial divergence operator and with

$$\boldsymbol{Q} = \boldsymbol{H}^T\boldsymbol{q} = -\boldsymbol{H}^T\boldsymbol{k}\boldsymbol{\nabla}\theta. \tag{96}$$

The spatial gradient of θ (96) can be conveniently related to its material counterpart as

$$\boldsymbol{\nabla}\theta = \boldsymbol{F}^{-T}\boldsymbol{\nabla}\theta = J^{-1}\boldsymbol{H}\boldsymbol{\nabla}\theta. \tag{97}$$

Finally, introduction of (97) into (96) yields

$$\boldsymbol{Q} = -\boldsymbol{K}\boldsymbol{\nabla}\theta; \qquad \boldsymbol{K} = J^{-1}\boldsymbol{H}^T\boldsymbol{k}\boldsymbol{H}. \tag{98}$$

5. Thermo-Electro-Elastodynamics

The objective of this section is to present the variational formulation that will be used in order to develop an EM time integration scheme in Section 5.3.

5.1. Continuum formulation

In order to derive a suitable EM time integrator, we first study the conservation properties of a thermo-electro-elastic continuum controlled by the governing equations (2), (6) and (3)-(4). For this, we present a formulation in terms of the energy functional depending upon the electric displacement field $\boldsymbol{D}_0$, namely $\widehat{W}(\boldsymbol{C}, \boldsymbol{G}, C, \boldsymbol{D}_0, \eta)$ defined as in (**??**) in order to satisfy the material stability conditions in (**??**). In this case, the formulation relies on the following five weak forms:

$$\begin{aligned}
\mathcal{W}_{\boldsymbol{v}} &= \int_{\mathcal{B}_0} \left(\boldsymbol{v} - \dot{\boldsymbol{\phi}} \right) \cdot \rho_0 \boldsymbol{w}_{\boldsymbol{v}} \, dV = 0; \\
\mathcal{W}_{\boldsymbol{\phi}} &= \int_{\mathcal{B}_0} \rho_0 \dot{\boldsymbol{v}} \cdot \boldsymbol{w}_{\boldsymbol{\phi}} \, dV + \int_{\mathcal{B}_0} \boldsymbol{P} : \frac{1}{2} D\boldsymbol{F}[\boldsymbol{w}_{\boldsymbol{\phi}}] \, dV - \mathcal{W}_{\boldsymbol{\phi}}^{\text{ext}} = 0; \\
\mathcal{W}_{\varphi} &= \int_{\mathcal{B}_0} \boldsymbol{D}_0 \cdot \boldsymbol{\nabla}_0 w_{\varphi} \, dV - \mathcal{W}_{\varphi}^{\text{ext}} = 0; \\
\mathcal{W}_{\theta} &= \int_{\mathcal{B}_0} \left(\frac{d}{dt} \left(\theta \eta \right) w_{\theta} \, dV - \dot{\theta} \eta w_{\theta} \right) dV - \int_{\mathcal{B}_0} \boldsymbol{Q} \cdot \boldsymbol{\nabla}_0 w_{\theta} \, dV - \mathcal{W}_{\theta}^{\text{ext}} = 0,
\end{aligned} \tag{99}$$

where the external mechanical, electrical and thermal contributions are defined as

$$\begin{aligned}
\mathcal{W}_{\boldsymbol{\phi}}^{\text{ext}} &= \int_{\mathcal{B}_0} \boldsymbol{f}_0 \cdot \boldsymbol{w}_{\boldsymbol{\phi}} \, dV + \int_{\partial_{\boldsymbol{t}} \mathcal{B}_0} \boldsymbol{t}_0 \cdot \boldsymbol{w}_{\boldsymbol{\phi}} \, dA; \qquad \mathcal{W}_{\varphi}^{\text{ext}} = - \int_{\mathcal{B}_0} \rho_0^e w_{\varphi} \, dV - \int_{\partial_{\omega} \mathcal{B}_0} \omega_0^e w_{\varphi} \, dA \\
\mathcal{W}_{\theta}^{\text{ext}} &= \int_{\mathcal{B}_0} R_{\theta} w_{\theta} \, dV + \int_{\partial_Q \mathcal{B}_0} Q_{\theta} w_{\theta} \, dA.
\end{aligned} \tag{100}$$

Furthermore, in (99), $\boldsymbol{P}$, $\boldsymbol{E}_0$ and θ are defined in terms of the derivatives of the energy functional $\widehat{W}(\boldsymbol{C}, \boldsymbol{G}, C, \boldsymbol{D}_0, \theta)$ as in (**??**) and with $\{\boldsymbol{v}, \boldsymbol{\phi}, \varphi, \boldsymbol{D}_0, \theta\} \in \{\mathbb{V}^{\boldsymbol{\phi}}, \mathbb{V}^{\boldsymbol{\phi}}, \mathbb{V}^{\varphi}, \mathbb{V}^{\boldsymbol{D}_0}, \mathbb{V}^{\theta}\}$ and $\{\boldsymbol{w}_{\boldsymbol{v}}, w_{\varphi}, \boldsymbol{w}_{\boldsymbol{D}_0}, w_{\theta}\} \in \{\mathbb{V}^{\boldsymbol{\phi}}, \mathbb{V}_0^{\boldsymbol{\phi}}, \mathbb{V}_0^{\varphi}, \mathbb{V}^{\boldsymbol{D}_0}, \mathbb{V}_0^{\theta}\}$,

$$\begin{aligned}
\mathbb{V}^{\boldsymbol{\phi}} &= \left\{ \boldsymbol{\phi} \in H^1\left(\mathcal{B}_0; \mathbb{R}^3\right) \mid \boldsymbol{\phi} = \bar{\boldsymbol{\phi}} \text{ on } \partial_{\boldsymbol{\phi}} \mathcal{B}_0 \text{ and } J > 0 \ a.e \right\}; \qquad \mathbb{V}_0^{\boldsymbol{\phi}} = \left\{ \boldsymbol{\phi} \in H^1\left(\mathcal{B}_0; \mathbb{R}^3\right) \mid \boldsymbol{\phi} = \boldsymbol{0} \text{ on } \partial_{\boldsymbol{\phi}} \mathcal{B}_0 \right\}; \\
\mathbb{V}^{\varphi} &= \left\{ \theta \in H^1\left(\mathcal{B}_0; \mathbb{R}\right); \mid \varphi = \bar{\varphi} \text{ on } \partial_{\varphi} \mathcal{B}_0 \right\}; \qquad \mathbb{V}^{\varphi} = \left\{ \theta \in H^1\left(\mathcal{B}_0; \mathbb{R}\right); \mid \varphi = 0 \text{ on } \partial_{\varphi} \mathcal{B}_0 \right\}; \\
\mathbb{V}^{\theta} &= \left\{ \theta \in H^1\left(\mathcal{B}_0; \mathbb{R}\right) \mid \theta = \bar{\theta} \text{ on } \partial_{\theta} \mathcal{B}_0 \right\}; \qquad \mathbb{V}^{\theta} = \left\{ \theta \in H^1\left(\mathcal{B}_0; \mathbb{R}\right) \mid \theta = 0 \text{ on } \partial_{\theta} \mathcal{B}_0 \right\}; \\
\mathbb{V}^{\boldsymbol{D}_0} &= \left\{ \boldsymbol{D}_0 \in \mathbb{L}_2\left(\mathcal{B}_0; \mathbb{R}^3\right) \right\}.
\end{aligned} \tag{101}$$

5.2. Semidiscret in time: time integrator

Following the work of Simo [51], Gonzalez [26], Romero [47] and Betsch [9, 10] in the context of nonlinear elasticity and Franke et al. [22] in the context of thermoelasticity, the objective of this section is to propose an EM preserving time discretisation scheme for the weak forms in (99).

Let us consider a sequence of time steps $\{t_1, t_2, ..., t_n, t_{n+1}\}$, where t_{n+1} denotes the current

time step. From the weak forms in (99), the following implicit one-step time integrator is proposed

$$
\begin{aligned}
\left(\mathcal{W}_{\boldsymbol{v}}\right)_{\text{algo}} &= \int_{\mathcal{B}_0} \left(\boldsymbol{v}_{n+1/2} - \frac{\Delta \boldsymbol{\phi}}{\Delta t} \right) \cdot \rho_0 \boldsymbol{w}_{\boldsymbol{v}} \, dV = 0; \\
\left(\mathcal{W}_{\boldsymbol{\phi}}\right)_{\text{algo}} &= \int_{\mathcal{B}_0} \rho_0 \frac{\Delta \boldsymbol{v}}{\Delta t} \cdot \boldsymbol{w}_{\boldsymbol{\phi}} \, dV + \int_{\mathcal{B}_0} \boldsymbol{S}_{\text{algo}} : \frac{1}{2} (D\boldsymbol{C}[\boldsymbol{w}_{\boldsymbol{\phi}}])_{\text{algo}} \, dV - \left(\mathcal{W}_{\boldsymbol{\phi}}^{\text{ext}}\right)_{n+1/2} = 0; \\
\left(\mathcal{W}_{\varphi}\right)_{\text{algo}} &= \int_{\mathcal{B}_0} \boldsymbol{D}_{0_{n+1/2}} \cdot \boldsymbol{\nabla}_0 \delta\varphi \, dV + \int_{\mathcal{B}_0} \rho^e_{0_{n+1/2}} \delta\varphi \, dV - \left(\mathcal{W}_{\varphi}^{\text{ext}}\right)_{n+1/2} = 0; \\
\left(\mathcal{W}_{\boldsymbol{D}_0}\right)_{\text{algo}} &= \int_{\mathcal{B}_0} \delta \boldsymbol{D}_0 \cdot \left(\boldsymbol{E}_{0\text{algo}} + \boldsymbol{\nabla}_0 \varphi_{n+1/2} \right) \, dV = 0; \\
\left(\mathcal{W}_{\theta}\right)_{\text{algo}} &= \int_{\mathcal{B}_0} \left(\frac{\Delta \left(\theta\eta\right)}{\Delta t} w_\theta - \frac{\Delta \theta}{\Delta t} \eta_{\text{algo}} \right) w_\theta \, dV - \int_{\mathcal{B}_0} \boldsymbol{Q}_{n+1/2} \cdot \boldsymbol{\nabla}_0 w_\theta \, dV - \left(\mathcal{W}_{\theta}^{\text{ext}}\right)_{n+1/2} = 0.
\end{aligned}
\tag{102}
$$

5.3. semidiscrete ... thermo-elastodynamics

5.4. Finite Element implementation

As standard in finite elements, the domain $\mathcal{B}_0$ described in Section 2.1 and representing a thermo-elastic continuum is sub-divided into a finite set of non-overlapping elements $e \in \mathbb{E}$ such that

$$
\mathcal{B}_0 \approx \mathcal{B}_0^h = \bigcup_{e \in \mathbb{E}} \mathcal{B}_0^e. \tag{103}
$$

The unknown fields $\{\boldsymbol{v}, \boldsymbol{\phi}, \varphi, \boldsymbol{D}_0\theta\}$ in the semi-discrete weak forms $\left(\mathcal{W}_{\boldsymbol{v}}\right)_{\text{algo}}$, $\left(\mathcal{W}_{\boldsymbol{\phi}}\right)_{\text{algo}}$, $\left(\mathcal{W}_{\phi}\right)_{\text{algo}}$, $\left(\mathcal{W}_{\boldsymbol{D}_0}\right)_{\text{algo}}$and $\left(\mathcal{W}_{\theta}\right)_{\text{algo}}$ in (102) are discretised employing the following functional spaces $\mathbb{V}^{\boldsymbol{\phi}^h} \times \mathbb{V}^{\boldsymbol{\phi}^h} \times \mathbb{V}^{\varphi^h} \times \mathbb{V}^{\boldsymbol{D}_0^h} \times \mathbb{V}^{\theta^h}$ defined as

$$
\begin{aligned}
&\mathbb{V}^{\boldsymbol{\phi}^h} = \{\boldsymbol{\phi} \in \mathbb{V}^{\boldsymbol{\phi}}; \quad \boldsymbol{\phi}^h\big|_{\mathcal{B}_0^e} = \sum_{a=1}^{n^{\boldsymbol{\phi}}_{\text{node}}} N_a^{\boldsymbol{\phi}} \boldsymbol{\phi}_a\}; && \mathbb{V}^{\varphi^h} = \{\varphi \in \mathbb{V}^{\varphi}; \quad \varphi^h\big|_{\mathcal{B}_0^e} = \sum_{a=1}^{n^{\varphi}_{\text{node}}} N_a^{\varphi} \varphi_a\}; \\
&\mathbb{V}^{\boldsymbol{D}_0^h} = \{\boldsymbol{D}_0 \in \mathbb{V}^{\boldsymbol{D}_0}; \quad \boldsymbol{D}_0^h\big|_{\mathcal{B}_0^e} = \sum_{a=1}^{n^{\boldsymbol{D}_0}_{\text{node}}} N_a^{\boldsymbol{D}_0} \boldsymbol{D}_{0a}\}; && \mathbb{V}^{\theta^h} = \{\theta \in \mathbb{V}^{\theta}; \quad \theta^h\big|_{\mathcal{B}_0^e} = \sum_{a=1}^{n^{\theta}_{\text{node}}} N_a^{\theta} \theta_a\},
\end{aligned}
\tag{104}
$$

where for any field $\boldsymbol{\mathcal{Y}} \in \{\boldsymbol{\phi}, \varphi, \boldsymbol{D}_0, \theta\}$, $n^{\boldsymbol{\mathcal{Y}}}_{\text{node}}$ denotes the number of nodes per element of the discretisation associated with the field $\boldsymbol{\mathcal{Y}}$ and $N_a^{\boldsymbol{\mathcal{Y}}} : \mathcal{B}_0^e \to \mathbb{R}$, the a^{th} shape function used for the interpolation of $\boldsymbol{\mathcal{Y}}$. In addition, $\boldsymbol{\mathcal{Y}}_a$ represents the value of the field $\boldsymbol{\mathcal{Y}}$ at the a^{th} node of a given finite element. Similarly, following a Bubnov-Galerkin approach, the functional spaces for the test functions $\{\boldsymbol{w}_{\boldsymbol{v}}, \boldsymbol{w}_{\boldsymbol{\phi}}, w_\varphi, \boldsymbol{w}_{\boldsymbol{D}_0}, w_\theta\} \in \mathbb{V}_0^{\boldsymbol{\phi}^h} \times \mathbb{V}_0^{\boldsymbol{\phi}^h} \times \mathbb{V}_0^{\varphi^h} \times \mathbb{V}^{\boldsymbol{D}_0^h} \times \mathbb{V}_0^{\theta^h}$ are defined as

$$
\begin{aligned}
&\mathbb{V}_0^{\boldsymbol{\phi}^h} = \left\{ \forall \boldsymbol{\phi} \in \mathbb{V}^{\boldsymbol{\phi}^h}; \quad \boldsymbol{\phi} = \boldsymbol{0} \text{ on } \partial_{\boldsymbol{\phi}} \mathcal{B}_0 \right\}; && \mathbb{V}_0^{\varphi^h} = \left\{ \forall \varphi \in \mathbb{V}^{\varphi^h}; \quad \varphi = 0 \text{ on } \partial_{\varphi} \mathcal{B}_0 \right\}; \\
&\mathbb{V}_0^{\theta^h} = \left\{ \forall \theta \in \mathbb{V}^{\theta^h}; \quad \theta = 0 \text{ on } \partial_{\theta} \mathcal{B}_0 \right\}.
\end{aligned}
\tag{105}
$$

Even though the relation between the time derivative of $\boldsymbol{\phi}$ and the velocity field $\boldsymbol{v}$ is imposed in a weak sense (refer to the weak form $\mathcal{W}_{\boldsymbol{v}}$ in $(102)_a$), the consideration of equal functional spaces for both fields, namely $\boldsymbol{\phi} \in \mathbb{V}^{\boldsymbol{\phi}}$ and $\boldsymbol{v} \in \mathbb{V}^{\boldsymbol{\phi}}$ enables to conclude that $(102)_a$ holds strongly, namely

$$
\frac{\Delta \boldsymbol{\phi}}{\Delta t} = \boldsymbol{v}_{n+1/2}. \tag{106}
$$

Consideration of the functional spaces for $\{\boldsymbol{v}, \boldsymbol{\phi}, \theta\}$ and $\{\boldsymbol{w}_{\boldsymbol{v}}, \boldsymbol{w}_{\boldsymbol{\phi}}, w_\theta\}$ in (104) and (105) enables $\{(\mathcal{W}_{\boldsymbol{\phi}})_{\text{algo}}, (\mathcal{W}_\theta)_{\text{algo}}\}$ in (102) to be written in terms of their associated elemental residual contributions, namely

$$\begin{aligned} (\mathcal{W}_{\boldsymbol{\phi}})_{\text{algo}} &= \sum_{e=1}^{N} \boldsymbol{w}_{\boldsymbol{\phi}a} \cdot \boldsymbol{R}^{\boldsymbol{\phi}}_{a,e}; \qquad (\mathcal{W}_{\varphi})_{\text{algo}} = \sum_{e=1}^{N} w_{\varphi a} R^{\varphi}_{a,e}; \\ (\mathcal{W}_{\boldsymbol{D}_0})_{\text{algo}} &= \sum_{e=1}^{N} \boldsymbol{w}_{\boldsymbol{D}_0 a} \cdot \boldsymbol{R}^{\boldsymbol{D}_0}_{a,e}; \qquad (\mathcal{W}_{\theta})_{\text{algo}} = \sum_{e=1}^{N} w_{\theta a} R^{\theta}_{a,e}, \end{aligned} \tag{107}$$

where N denotes the number of elements for the underlying discretisation. The residual contributions $\boldsymbol{R}^{\boldsymbol{\phi}}_{a,e}$, $R^{\varphi}_{a,e}$, $\boldsymbol{R}^{\boldsymbol{D}_0}_{a,e}$ and $R^{\theta}_{a,e}$ can be expressed as[12]

$$\begin{aligned} \boldsymbol{R}^{\boldsymbol{\phi}}_{a,e} &= \int_{\mathcal{B}^e_0} \rho_0 N^a_{\boldsymbol{\phi}} \left(2\frac{\Delta \boldsymbol{\phi}}{\Delta t^2} - 2\frac{\boldsymbol{v}_n}{\Delta t} \right) dV + \int_{\mathcal{B}^e_0} \left(\boldsymbol{F}_{n+1/2} \boldsymbol{S}_{\text{algo}} \right) \boldsymbol{\nabla}_0 N^{\boldsymbol{\phi}}_a \, dV + \int_{\mathcal{B}^e_0} N^{\boldsymbol{\phi}}_a \boldsymbol{f}_{0_{n+1/2}} \, dV; \\ R^{\varphi}_{a,e} &= \int_{\mathcal{B}_0} \boldsymbol{D}_{0_{n+1/2}} \cdot \boldsymbol{\nabla}_0 N^{\varphi}_a \, dV + \int_{\mathcal{B}_0} \rho^e_{0_{n+1/2}} N^{\varphi}_a \, dV; \\ (\mathcal{W}_{\boldsymbol{D}_0})_{\text{algo}} &= \int_{\mathcal{B}_0} \left(\boldsymbol{E}_{0\text{algo}} + \boldsymbol{\nabla}_0 \varphi_{n+1/2} \right) N^{\boldsymbol{D}_0}_a \, dV; \\ R^{\theta}_{a,e} &= \int_{\mathcal{B}_0} \frac{\Delta \left(\theta \eta \right)}{\Delta t} N^{\theta}_a \, dV - \int_{\mathcal{B}_0} \frac{\Delta \theta}{\Delta t} \eta_{\text{algo}} N^{\theta}_a \, dV - \int_{\mathcal{B}_0} \boldsymbol{Q}_{n+1/2} \cdot \boldsymbol{\nabla}_0 N^{\theta}_a \, dV - \int_{\mathcal{B}_0} R_{\theta n+1/2} N^{\theta}_a \, dV. \end{aligned} \tag{108}$$

where use of equation (106) has been made of in the inertial term of the residual $\boldsymbol{R}^{\boldsymbol{\phi}}_{a,e}$ in $(108)_a$. A consistent linearisation of the nonlinear residual contributions (108) has been used in this work.

6. Model calibration

The constitutive model presented in section 3 is general and can be applied to a wide variety of materials. In the context of EAPs, multiple authors have performed experimental testing, of the single physics, such as mechanical, thermal or electrical behaviour ([20, 31]) as well as the coupled behaviour of the combination of two ([1, 38]) or the three physics ([40, 46, 50]). The data reported in the literature will be used to calibrate a constitutive model for VHB polymer, where the calibration involves the choice of specific mechanical models and thermal functions, fitting the best parameters and estimating an error for the model.

Beyond finding optimal parameters, the scope of the calibration is to validate the theoretical formulation and to show its capabilities. The proposed framework is valid for other materials and the methodology shows some conclusions that can be applied for other material characterization.

6.1. Experiment and data availability

For the accurate calibration of VHB polymer, data from the literature has been collected and classified. The selected experimental tests can be classified in the following groups: differential scanning calorimetry (DSC), one-cycle loading-unloading tests, creep tests at constant deformation, quasi-static loading and broadband dielectric spectrometry (BDS). Mechanical as well as electrical tests provide data at different temperatures, covering a range from $-20°$C up to $80°$C.

[12] For simplicity, the external contributions on the boundary of the continuum and associated with $\boldsymbol{t}_0$ and Q_θ have not been included in (108).

Some of the tests are very specific and allow to calibrate a single parameter of a very narrow set of parameters. Other tests like cyclic loading involve the coupling of the thermal, elastic and viscous effects.

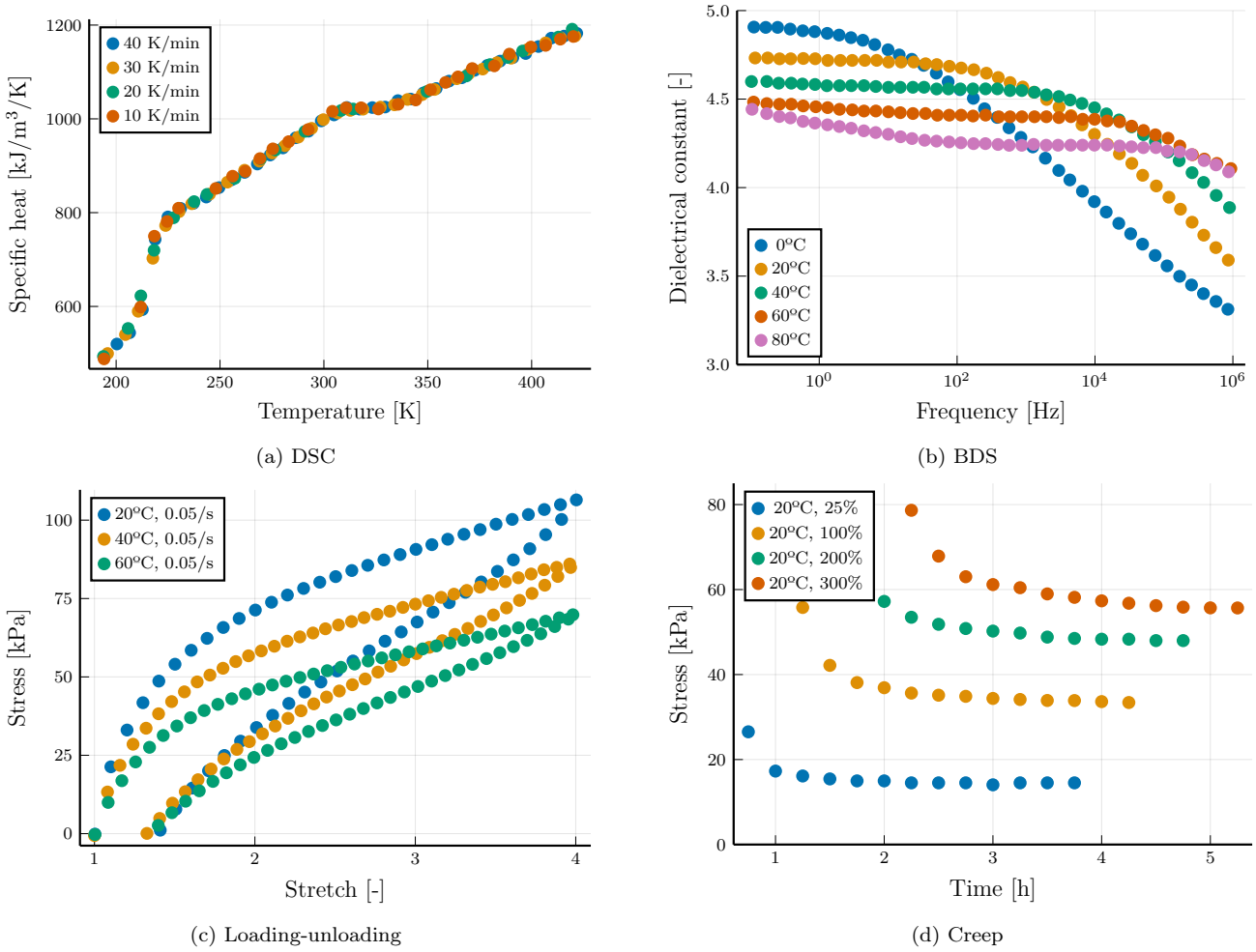

(a) DSC (b) BDS

(c) Loading-unloading (d) Creep

Figure 3: Visualization of selected experiments showing the thermo-electro-mechanical response of the material.

The most relevant experiments that will be used in the calibration of the constitutive model are shown in figure (3). DSC and BDS experiments follow standardized protocols and more information can be found in [32] and [34] respectively. This two experiments allow to identify specific heat and dielectric properties in the absence of mechanical actions.

Finally, an important consideration is that the stresses on uniaxial experiments reported by different authors under the same conditions of temperature, velocity and stretch may be different. This observation would open a discussion about uncertainty of the material data and error propagation. Given the scope of this investigation is to assess the suitability of the numerical model to predict the behaviour of EAPs, only consistent data will be considered. There are several potential sources for the differences of the measured properties: VHB polymer is manufactured as an adhesive tape, hence, quality control focus on properties different from viscoelastic behaviour; VHB polymer is provided in different thicknesses, which can alter the curing process of the polymer; and finally, engineering tolerances are not defined for the current properties and can suffer variations from one batch of production to another one.

Table 1: Types and sources of experimental data.

Data Set	Experiment Type	Reference
Set 1	Differential scanning calorimetry (DSC)	[20]
Set 2	One-cycle loading-unloading	[38]
Set 3	Constant stretch creep	[38]
Set 4	Quasi-static loading	[38]
Set 5	One-cycle loading-unloading (discarded)	[1]
Set 6	Constant stretch creep (discarded)	[1]
Set 7	Broadband dielectric spectroscopy (BDS)	[50]
Set 8	Thermo-electro-mechanical one-cycle loading-unloading	[40]

6.2. Uniaxial experiments loading protocol

Mechanical tests gather some families of experiments, such as cyclic loading, quasi-static loading, and creep at constant stretch. Quasi-static tests are a subtype of cyclic loading at a very low velocity and coincide with the asymptotic stress of the creep tests. These experiments are widely used for the mechanical characterization of viscoelastic materials, however, they are not standardized and the loading protocols can be vary across laboratories and authors. Understanding the loading protocols is needed to define the numerical simulation of experiments and thus, to perform an optimization for the material parameters.

6.2.1. Kinematics

The mechanical tests reported in [1, 38] describe the following protocol: First, the specimens were placed inside the chamber and conditioned at the target temperature for fifteen minutes to achieve thermal homogeneity across the 0 5mm thickness. Crucially, the specimens were mounted onto the grippers only after this thermal stabilization period. The protective silicon paper was then removed gently to ensure the test initiated without any pre-tension. Consequently, the reference configuration for each experiment—corresponding to a stretch of $\lambda = 1$ and zero nominal stress—is defined by the stress-free state of the material after free thermal expansion or contraction at the specific test temperature. The mechanical response was recorded as the Piola (nominal) stress, calculated by dividing the applied force by the initial undeformed cross-sectional area measured at the start of the test. Accordingly, the deformation gradient tensor is straightforwardly found as the composition of volumetric and isochoric parts as

$$\boldsymbol{F}_{TM1} = \bar{\boldsymbol{F}}\hat{\boldsymbol{F}} = (1 + \alpha(\theta - \theta_R))^{1/3} \begin{bmatrix} \lambda & 0 & 0 \\ 0 & \lambda^{-1/2} & 0 \\ 0 & 0 & \lambda^{-1/2} \end{bmatrix}, \tag{109}$$

where α is the volumetric thermal expansion coefficient.

On the other hand, In thermo-electromechanical scenarios [40], the mounted specimen was placed in the temperature-controlled chamber and allowed to reach thermal equilibrium for 15 minutes before loading. The loading sequence was strictly defined: first, a constant electric potential (2 kV to 6 kV) was applied across the thickness. The material was held under this pure electrical load for one minute to stabilize initial deformations. Due to the electric-field-induced expansion being constrained by the fixed clamps, the force measured at the nominal 0% stretch typically initiated at a slight compressive (negative) value. In the absence of electrical field, the

deformation gradient would be expressed according to

$$\boldsymbol{F}_{TM2} = \begin{bmatrix} \lambda & 0 & 0 \\ 0 & (J/\lambda)^{1/2} & 0 \\ 0 & 0 & (J/\lambda)^{1/2} \end{bmatrix} \; ; \quad J = 1 - \alpha(\theta - \theta_R)\,. \tag{110}$$

It is important to remark that, unlike (109), (110) is linked with non-zero axial stresses for $\lambda = 1$ at temperatures different from θ_R. Given the electrical field will introduce a transverse deformation λ_2, the kinematics will follow the expressions

$$\boldsymbol{F}_{TEM} = \begin{bmatrix} \lambda & 0 & 0 \\ 0 & J^{1/2}\lambda_2 & 0 \\ 0 & 0 & J^{1/2}(\lambda\lambda_2)^{-1} \end{bmatrix} \; , \quad \boldsymbol{E} = \begin{bmatrix} 0 \\ V/T_0 \\ 0 \end{bmatrix} \tag{111}$$

where T_0 is the reference undeformed thickness and λ_2 must be such that the transverse stresses P_{22} and P_{33} equal to zero.

6.2.2. First Piola-Kirchhoff stress

The process of the calibration of a constitutive model involves the simulation of the experiments and how the constitutive model is able to predict the stress for the series of stretches in each experiment. The aforementioned deformation gradients define the kinematics of the specimen and the evaluation of the stress must be closed with appropriate boundary conditions (i.e., a traction-free state on the lateral surfaces of the specimen) by the addition of a hydrostatic pressure. The total Piola-Kirchhoff stress is given by $\boldsymbol{P} = \boldsymbol{P}^{\text{dev}} - pJ\boldsymbol{F}^{-T}$. Given that the lateral components must vanish ($P_{22} = P_{33} = 0$), the pressure p is coupled to the constitutive response as:

$$p = P_{22}^{\text{dev}} F_{22} \tag{112}$$

Consequently, the axial stress used in the objective function of the model calibration is computed as:

$$P_{11} = P_{11}^{\text{dev}} - pF_{11}^{-1} = P_{11}^{\text{dev}} - P_{22}^{\text{dev}} \frac{F_{22}}{F_{11}} \tag{113}$$

6.3. Constitutive model calibration

The material parameters for the constitutive were identified by minimizing the discrepancy between the experimental data and the theoretical response for each experiment type. For every experiment, the objective function is defined as the L_2 norm of the dimensionless error.

6.4. Validation and error estimation

6.5. Conclusions

7. Numerical examples

8. Conclusions

9. Acknowledgements

The first author acknowledges the support provided by Ministerio de Ciencia, Innovación y Universidades, for the award of a Juan de la Cierva Formación Fellowship. The first and third author acknoledge the support of AEI/FEDER and UE under the contracts DPI2016-77538-R and by the Fundacion Séneca (Agencia de Ciencia y Tecnología de la Región de Murcia (Spain)) under the contract 20911/PI/18. The second author acknowledges the financial support received through the European Training Network Protection (Project ID: 764636).

References

[1] Keven Alkhoury, Nikola Bosnjak, Yueping Wang, Howon Lee, Siva Nadimpalli, and Shawn A. Chester. Experiments and modeling of the thermo-mechanically coupled behavior of vhb. *International Journal of Solids and Structures*, 242:111523, 2022.

[2] Lallit Anand. Constitutive equations for hot-working of metals. *International Journal of Plasticity*, 1(3):213–231, 1985.

[3] J. M. Ball. Convexity conditions and existence theorems in nonlinear elasticity. *Archive for Rational Mechanics and Analysis*, 63(4):337–403, 1976.

[4] J. M. Ball. Energy-minimising configurations in nonlinear elasticity. *Archive for Rational Mechanics and Analysis*, 63(4):337–403, 1976.

[5] J. M. Ball. *Geometry, Mechanics and Dynamics*, chapter Some open problems in Elasticity, pages 3–59. Springer, 2002.

[6] J. M. Ball and F. Murat. $W^{1,p}$-quasiconvexity and variational problems for multiple integrals. *Journal of Functional Analysis*, 58(3):225–253, 1984.

[7] J.S. Bergström and M.C. Boyce. Constitutive modeling of the large strain time-dependent behavior of elastomers. *Journal of the Mechanics and Physics of Solids*, 46(5):931–954, 1998.

[8] K. Bertoldi and M. Gei. Instabilities in multilayered soft dielectrics. *Journal of the Mechanics and Physics of Solids*, 59(1):18–42, 2011.

[9] P. Betsch and A. Janz. An energy-momentum consistent method for transient simulations with mixed finite elements developed in the framework of geometrically exact shells. *Int. J. Numer. Meth. Engng*, 108(5):423–455, 2016.

[10] P. Betsch, A. Janz, and C. Hesch. A mixed variational framework for the design of energy-momentum schemes inspired by the structure of polyconvex stored energy functions. *Computer Methods in Applied Mechanics and Engineering*, 335:660–696, 2018.

[11] J. Bonet. Large strain viscoelastic constitutive models. *International Journal of Solids and Structures*, 38(17):2953–2968, 2001.

[12] J. Bonet, A. J. Gil, C. H. Lee, M. Aguirre, and R. Ortigosa. A first order hyperbolic framework for large strain computational solid dynamics - Part I: Total Lagrangian isothermal elasticity. *Computer Methods in Applied Mechanics and Engineering*, 283(0):689–732, 2015.

[13] J. Bonet, A. J. Gil, and R. Ortigosa. A computational framework for polyconvex large strain elasticity. *Computer Methods in Applied Mechanics and Engineering*, 283:1061–1094, 2015.

[14] J. Bonet, A. J. Gil, and R. Ortigosa. On a tensor cross product based formulation of large strain solid mechanics. *International Journal of Solids and Structures*, 84:49–63, 2016.

[15] J. Bonet, A. J. Gil, and R. D. Wood. *Nonlinear Continuum Mechanics for Finite Element Analysis: Statics*. Cambridge University Press, 2016.

[16] Javier Bonet and Antonio J. Gil. Finite strain thermoelasticity and the third law of thermodynamics. *Journal of the Mechanics and Physics of Solids*, 206:106372, 2026.

[17] Javier Bonet and Antonio J. Gil. Finite strain thermoelasticity and the third law of thermodynamics. *Journal of the Mechanics and Physics of Solids*, 206:106372, 2026.

[18] R. Bustamante, A. Dorfmann, and R.W. Ogden. On electric body forces and Maxwell stresses in nonlinearly electroelastic solids. *International Journal of Engineering Science*, 47(11-12):1131–1141, 2009.

[19] R. de Boer. *Vektor- und Tensorrechnung für Ingenieure*. Springer-Verlag, 1982.

[20] B. Dippel, M. Johlitz, and A. Lion. Thermo-mechanical couplings in elastomers – experiments and modelling. *ZAMM - Journal of Applied Mathematics and Mechanics / Zeitschrift für Angewandte Mathematik und Mechanik*, 95(11):1117–1128, 2015.

[21] A. Dorfmann and R. W. Ogden. Nonlinear electroelasticity. *Acta Mechanica*, 174(3-4):167–183, 2005.

[22] M Franke, A. Janz, M. Schiebl, and P. Betsch. An energy momentum consistent integration scheme using a polyconvexity-based framework for nonlinear thermo-elastodynamics. *International Journal for Numerical Methods in Engineering*, 115:549–577, 2018.

[23] M. Franke, R. Ortigosa, A. Janz, A.J. Gil, and P. Betsch. A mixed variational framework for the design of energy–momentum integration schemes based on convex multi-variable electro-elastodynamics. *Computer Methods in Applied Mechanics and Engineering*, 351:109–152, 2019.

[24] M. Franke, R. Ortigosa, J. Martínez-Frutos, A.J. Gil, and P. Betsch. A thermodynamically consistent time integration scheme for non-linear thermo-electro-mechanics. *Computer Methods in Applied Mechanics and Engineering*, 389:114298, 2022.

[25] A. J. Gil and R. Ortigosa. A new framework for large strain electromechanics based on convex multi-variable strain energies: variational formulation and material characterisation. *Computer Methods in Applied Mechanics and Engineering*, 302:293–328, 2016.

[26] O. Gonzalez. Exact energy and momentum conserving algorithms for general models in nonlinear elasticity. *Comput. Methods Appl. Mech. Engrg.*, 190:1763–1783, 2000.

[27] O. Gonzalez and A. M. Stuart. *A first course in Continuum Mechanics*. Cambridge University Press, 2008.

[28] M. Groß and P. Betsch. Energy-momentum consistent finite element discretization of dynamic finite viscoelasticity. *Int. J. Numer. Meth. Engng*, 81(11):1341–1386, 2010.

[29] M. E. Gurtin, E. Fried, and L. Anand. *The Mechanics and Thermodynamics of Continua*. Cambridge University Press, 2010.

[30] Hagen Holthusen, Christiane Rothkranz, Lukas Lamm, Tim Brepols, and Stefanie Reese. Inelastic material formulations based on a co-rotated intermediate configuration—application to bioengineered tissues. *Journal of the Mechanics and Physics of Solids*, 172:105174, 2023.

[31] Mokarram Hossain, Duc Khoi Vu, and Paul Steinmann. Experimental study and numerical modelling of vhb 4910 polymer. *Computational Materials Science*, 59:65–74, 2012.

[32] G. W. H. Höhne, W. F. Hemminger, and H.-J. Flammersheim. *Differential Scanning Calorimetry*. Springer-Verlag, 2003.

[33] G. Kofod, P. Sommer-Larsen, R. Kornbluh, and R. Pelrine. Actuation response of polyacrylate dielectric elastomers. *Journal of Intelligent Material Systems and Structures*, 14(12):787–793, 2003.

[34] Friedrich Kremer and Andreas Schönhals, editors. *Broadband Dielectric Spectroscopy*. Springer-Verlag, Berlin, Heidelberg, 2003.

[35] Ekkehart Kröner. Allgemeine kontinuumstheorie der versetzungen und eigenspannungen. *Archive for Rational Mechanics and Analysis*, 4(1):273–334, 1959.

[36] E. H. Lee. Elastic-plastic deformation at finite strains. *Journal of Applied Mechanics*, 36(1):1–6, 03 1969.

[37] T. Li, C. Keplinger, R. Baumgartner, S. Bauer, W. Yang, and Z. Suo. Giant voltage-induced deformation in dielectric elastomers near the verge of snap-through instability. *Journal of the Mechanics and Physics of Solids*, 61(2):611–628, 2013.

[38] Zisheng Liao, Mokarram Hossain, Xiaohu Yao, Markus Mehnert, and Paul Steinmann. On thermo-viscoelastic experimental characterization and numerical modelling of vhb polymer. *International Journal of Non-Linear Mechanics*, 118:103263, 2020.

[39] S. C. Martín and J. C. García Orden. On energy-entropy-momentum integration methods for discrete thermo-visco-elastodynamics. *Computers & Structures*, 181:3–20, 2017. UK Association of Computational Mechanics.

[40] Markus Mehnert, Mokarram Hossain, and Paul Steinmann. A complete thermo-electro-viscoelastic characterization of dielectric elastomers, part i: Experimental investigations. *Journal of the Mechanics and Physics of Solids*, 157:104603, 2021.

[41] Markus Mehnert, Mokarram Hossain, and Paul Steinmann. A complete thermo-electro-viscoelastic characterization of dielectric elastomers, part ii: Continuum modeling approach. *Journal of the Mechanics and Physics of Solids*, 157:104625, 2021.

[42] R. Ortigosa, M. Franke, A. Janz, A.J. Gil, and P. Betsch. An energy–momentum time integration scheme based on a convex multi-variable framework for non-linear electro-elastodynamics. *Computer Methods in Applied Mechanics and Engineering*, 339:1–35, 2018.

[43] R. Ortigosa, A.J. Gil, J. Martínez-Frutos, M. Franke, and J. Bonet. A new energy–momentum time integration scheme for non-linear thermo-mechanics. *Computer Methods in Applied Mechanics and Engineering*, 372:113395, 2020.

[44] R. Pelrine, R. Kornbluh, Q. Pei, and J. Joseph. High-speed electrically actuated elastomers with strain greater than 100 %. *Science*, 287(5454):836–839, 2000.

[45] R. E. Pelrine, R. D. Kornbluh, and J. P. Joseph. Electrostriction of polymer dielectrics with compliant electrodes as a means of actuation. *Sensors and Actuators A: Physical*, 64(1):77–85, 1998.

[46] Bao Qin, Zheng Zhong, and Tong-Yi Zhang. A thermo-electro-viscoelastic model for dielectric elastomers. *Materials*, 16(17), 2023.

[47] I. Romero. An analysis of the stress formula for energy-momentum methods in nonlinear elastodynamics. *Computational Mechanics*, 50(5):603–610, Nov 2012.

[48] J. Schröder. Anisotropic polyconvex energies. In J. Schröder and P. Neff, editors, *Poly-, quasi- and rank-one convexity in Applied Mechanics, volume 516 of CISM Courses and Lectures*, volume 516 of CISM Courses and Lectures, pages 53–105. Springer-Verlag, 2010.

[49] J. Schröder, P. Neff, and D. Balzani. A variational approach for materially stable anisotropic hyperelasticity. *International Journal of Solids and Structures*, 42:4352–4371, 2005.

[50] Junjie Sheng, Hualing Chen, Junhua Qiang, Bo Li, and Yongquan Wang. Thermal, mechanical, and dielectric properties of a dielectric elastomer for actuator applications. *Journal of Macromolecular Science, Part B*, 51(10):2093–2104, 2012.

[51] J. C. Simo and N. Tarnow. The discrete energy-momentum method. Conserving algorithms for nonlinear elastodynamics. *Zeitschrift für angewandte Mathematik und Physik ZAMP*, 43(5):757–792, Sep 1992.

[52] J.C. Simo. On a fully three-dimensional finite-strain viscoelastic damage model: Formulation and computational aspects. *Computer Methods in Applied Mechanics and Engineering*, 60(2):153–173, 1987.

[53] J.C. Simo. A framework for finite strain elastoplasticity based on maximum plastic dissipation and the multiplicative decomposition: Part i. continuum formulation. *Computer Methods in Applied Mechanics and Engineering*, 66(2):199–219, 1988.

[54] J.C. Simo and C. Miehe. Associative coupled thermoplasticity at finite strains: Formulation, numerical analysis and implementation. *Computer Methods in Applied Mechanics and Engineering*, 98(1):41–104, 1992.

[55] Juan C. Simo and Robert L. Taylor. Quasi-incompressible finite elasticity in principal stretches. continuum basis and numerical algorithms. *Computer Methods in Applied Mechanics and Engineering*, 85(3):273–310, 1991.

[56] S. Skatulla, C. Sansour, and A. Arockiarajan. A multiplicative approach for nonlinear electroelasticity. *Computer Methods in Applied Mechanics and Engineering*, 245-246(0):243–255, 2012.

[57] Rocco Vertechy, Giovanni Berselli, Vincenzo Parenti Castelli, and Massimo Bergamasco. Continuum thermo-electro-mechanical model for electrostrictive elastomers. *Journal of Intelligent Material Systems and Structures*, 24(6):761–778, 2013.

[58] D. K. Vu and P. Steinmann. On 3-D coupled BEM-FEM simulation of nonlinear electroelastostatics. *Computer Methods in Applied Mechanics and Engineering*, 201-204(0):82–90, 2012.